




REVIEW ARTICLE | FEBRUARY 17 2023

Visible-light photoredox catalysis with organic polymers

Gaurav Kumar; Bin Cai; Sascha Ott ; Haining Tian  



Chem. Phys. Rev. 4, 011307 (2023)

<https://doi.org/10.1063/5.0123282>



CrossMark



AIP Advances

Why Publish With Us?



25 DAYS

average time
to 1st decision



740+ DOWNLOADS

average per article



INCLUSIVE

scope

[Learn More](#)

 AIP
Publishing

Visible-light photoredox catalysis with organic polymers

Cite as: Chem. Phys. Rev. **4**, 011307 (2023); doi: [10.1063/5.0123282](https://doi.org/10.1063/5.0123282)

Submitted: 29 August 2022 · Accepted: 30 December 2022 ·

Published Online: 17 February 2023



View Online



Export Citation



CrossMark

Gaurav Kumar, Bin Cai, Sascha Ott,  and Haining Tian^{a)} 

AFFILIATIONS

Department of Chemistry—Ångström Laboratory, Uppsala University, 751 20 Uppsala, Sweden

^{a)} Author to whom correspondence should be addressed: haining.tian@kemi.uu.se

ABSTRACT

The development of photocatalysts to drive organic reactions is a frontier research topic. Organic polymers can be well tuned in terms of structural and photophysical properties and, therefore, constitute a promising class of photocatalysts in photoredox catalysis for organic synthesis. In this review article, we provide an overview of the concept of photoredox catalysis and recent developments in organic polymers as photocatalysts including porous organic polymers, graphitic carbon nitride, carbon dots, and polymer dots with adjustable reactivity that have undergone state-of-the-art advancement in different photoredox catalytic organic reactions.

© 2023 Author(s). All article content, except where otherwise noted, is licensed under a Creative Commons Attribution (CC BY) license (<http://creativecommons.org/licenses/by/4.0/>). <https://doi.org/10.1063/5.0123282>

TABLE OF CONTENTS

I. INTRODUCTION	1
II. PHOTOPHYSICS AND PHOTOCHEMISTRY	2
A. Molecular photocatalysts	2
B. Polymeric photocatalysts	3
III. PHOTOREACTION	3
IV. MECHANISTIC APPROACH FOR PHOTOREDOX CATALYSIS	4
A. Net oxidative reactions	4
B. Net reductive reactions	4
C. Redox neutral reactions	4
V. ORGANIC POLYMERIC PHOTOCATALYSTS FOR PHOTOREDOX CATALYSIS	4
A. Porous organic polymers (POPs)	4
B. Design principles	6
C. Design strategy	6
1. Oxidation reaction	7
2. Coupling reactions	13
3. Porous organic polymer photoisomerization of olefins	13
4. Reductions reactions	13
D. g-C ₃ N ₄	14
1. Characteristics of the g-C ₃ N ₄	14
2. Oxidation reaction	15
3. sp ³ C–H activation	15
4. Suzuki coupling reaction	18
E. Carbon dots	18

1. Characteristics of carbon dots	18
2. Oxidation reactions	18
3. Reduction reactions	19
F. Polymer dots	19
VI. PERSPECTIVE	20

I. INTRODUCTION

Photocatalysts that absorb photon energy and drive reactions have been widely used for hydrogen production,^{1–3} CO₂ reduction,⁴ water treatment⁵ and phototherapy.⁶ This technology converts solar energy directly into chemical energy.^{7–10} Recently, using photocatalysis to drive organic reactions has also been rapidly developed and is commonly recognized as “photoredox catalysis.” The term photoredox catalysis was coined as early as 1911.¹¹ As the photocatalyst is at the core of photoredox catalysis, the development of photocatalysts to drive various reactions is, therefore, desirable.

Inorganic semiconductors, such as TiO₂, CdSe, WO₃, ZnS, and ZnO,^{12,13} have been used as photocatalysts to drive organic reactions. Due to large band gaps, most of them only absorb UV regions. Metal complexes, such as ruthenium and iridium complexes,^{14–17} can absorb visible light; however, their scarcity and toxicity hampers their industrial application. Small organic molecular photocatalysts, such as fluorescein and rose bengal,^{18–20} have been used in some photoredox catalytic reactions and showed good reactivity. However, the reactions using small organic molecular photocatalysts are commonly carried

out under homogenous conditions, which makes the recycling of photocatalysts difficult.

Over the past decade, we have witnessed a swift gain in the advance of heterogeneous organic photocatalysts, such as organic polymeric photocatalysts for photoredox catalysis. Organic polymers are considered a promising type of photocatalyst for organic synthesis owing to their good light-harvesting ability, high strength, and modularity, easy accessibility to building blocks, abundance of active sites, feasible recycling process after photocatalysis, etc.^{21–27} In this review, we will overview the fundamental working principle of photoredox catalysis and the applications of organic polymeric photocatalysts, including porous organic polymers (POPs), graphitic carbon nitride (g-C₃N₄), carbon dots (Cdots), and polymer dots (Pdots), in various photoredox catalytic reactions such as coupling, reduction, and oxidation.

II. PHOTOPHYSICS AND PHOTOCHEMISTRY

A. Molecular photocatalysts

Basic photochemistry knowledge is fundamental to understand the working principle of a photoredox catalytic reaction. As shown in the simplified Jablonski diagram Fig. 1, the electron in a photocatalyst is prompted from its ground state (S_0) to the first singlet state (S_1) upon light absorption which normally happens on the timescale of femtoseconds, followed by rapid vibrational relaxation to the lowest vibrational energy level in S_1 state.²⁸ Thus, the prompted electron or/and the created holes play a crucial role in later catalytic reactions before the electron and hole are recombined by emitting fluorescence or via internal conversion. However, the formation of a triplet state (T_1) via intersystem cross (ISC) from the S_1 state could be also helpful for some photocatalytic reactions.²⁹ Because the deactivation of T_1 state to S_0 state via phosphorescence is spin-forbidden, T_1 is relatively

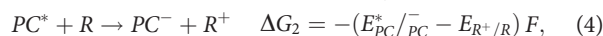
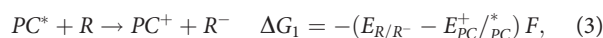
long-lived as compared to the S_1 state. Thus, the T_1 state, in principle, is more favorable to certain reactions which take charges from the photocatalyst rather slowly, if the charge transfer between the T_1 state of the photocatalyst and the substance is still thermodynamically feasible. The reduction and oxidation potentials of an excited state can be obtained from the following formulas:

$$E_{PC^*/PC}^* = E_{PC/PC^-} + E_{0-0}, \quad (1)$$

$$E_{PC^+/PC}^* = E_{PC^+/PC}^+ - E_{0-0}, \quad (2)$$

where PC^* is the excited photocatalyst, E_{PC^*/PC^-} is the reduction potential of the excited-state photocatalyst, E_{PC/PC^-} is the reduction potential of the ground-state photocatalyst, E_{0-0} is the 0–0 transition energy of the photocatalyst; E_{PC^+/PC^*} is the oxidation potential of the excited-state photocatalyst, and $E_{PC^+/PC}$ is the oxidation potential of the ground-state photocatalyst.

The reactant can either be reduced or oxidized by the excited photocatalyst depending on their relative redox potentials, the following reactions may happen:



where R is the reactant substrate, R^- is the reduced state of the reactant, ΔG_1 is the reaction Gibbs free energy when the reactant is reduced by the excited photocatalyst, F is the Faraday constant, R^+ is the oxidized state of the reactant, E_{R/R^-} is the reduction potential of the reactant, $E_{R^+/R}$ is the oxidation potential of the reactant, and ΔG_2 is the reaction Gibbs free energy when the reactant is oxidized by the excited photocatalyst.

Assuming that all reduction and oxidation processes are only one electron involved, then the reaction Gibbs free energy is listed as

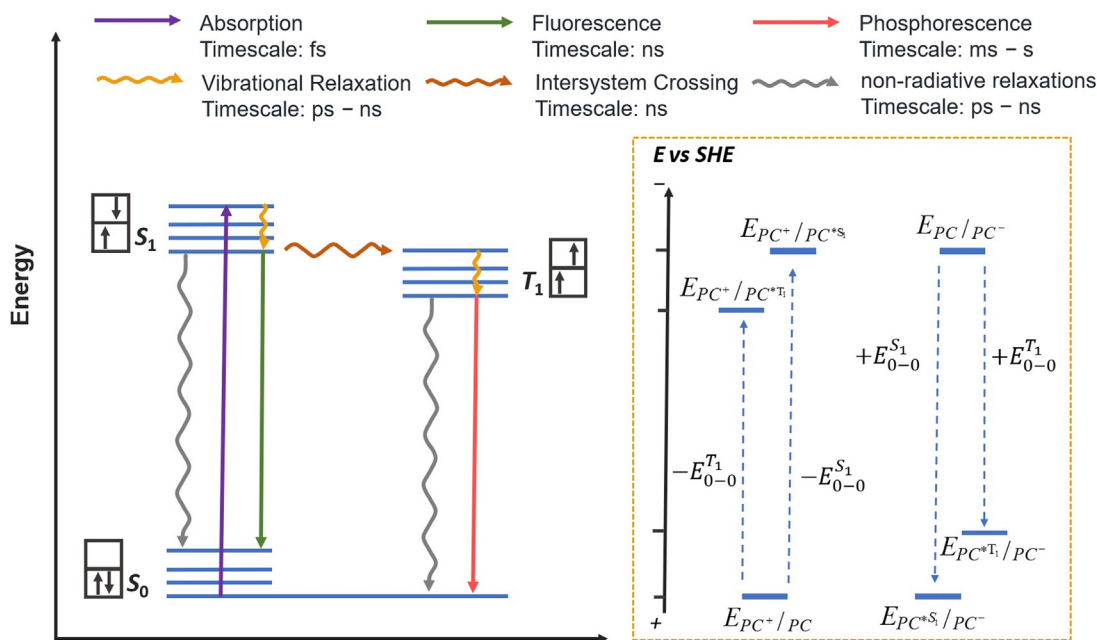


FIG. 1. Jablonski diagram of creating an excited singlet state and triplet state of the photocatalysts (PC) and their relative redox potentials.

formula (3) and (4). In order to ensure $\Delta G_1 < 0$ during a photo-reduction process, $E_{PC/PC}^{+/*} < E_{R/R}^-$ should be fulfilled. Similarly, in order to guarantee $\Delta G_2 < 0$ during a photo-oxidation process, $E_{PC/PC}^{+/*} > E_{R/R}^+$ should be satisfied.³⁰

E_{0-0} is normally determined by the intersection wavelength (λ_{int}) between absorption and emission spectra of the photocatalyst,

$$E_{0-0} = hc/\lambda_{int} = 1240/\lambda_{int}, \quad (5)$$

where h is Planck's constant and c is the speed of light.

B. Polymeric photocatalysts

Since polymers are used as alternative photocatalysts, many methods have been used to determine the energy levels and bandgap of the polymer. The above method for molecular photocatalysts has also been applied to polymers when the polymers are treated as molecules.² The oxidation potential of a polymer obtained from electrochemistry or ultraviolet photoelectron spectroscopy (UPS) is also commonly used as the polymer's highest-occupied molecular orbital (HOMO) or valence band (VB) edge.^{31,32} The lowest unoccupied molecular orbital (LUMO) or conduction band (CB) edge can be calculated from the bandgap (E_g) of the polymer,

$$E_g = \text{HOMO} - \text{LUMO} = E_{VB} - E_{CB}, \quad (6)$$

where E_{VB} and E_{CB} are the energy of VB and CB edge of the polymers.

In some cases, HOMO and LUMO levels of a polymer are directly taken from oxidation and reduction potential from cyclic voltammetry, respectively.^{33,34} E_g that are determined in that fashion may however be flawed by considerable mistakes as most polymers exhibit electrochemically irreversible oxidations and reductions, and the anodic and cathodic peak potentials do not reflect the true thermodynamic potentials. In addition to electrochemistry, the onset wavelength of the absorption spectrum [Eq. (7)] and the Tauc plot [Eq. (8)] is also used to determine E_g of the polymer,

$$E_g = hc/\lambda_{onset} = 1240/\lambda_{onset}, \quad (7)$$

where h is Planck's constant, c is the speed of light, and λ_{onset} is the onset wavelength of the absorption spectrum,

$$(\alpha h\nu)^n = A(h\nu - E_g), \quad (8)$$

where α is the molar absorption coefficient, $h\nu$ is the photon energy, A is the proportionality constant (i.e., based on refraction index, effective masses of electron and hole; however, for amorphous materials it is considered to be 1), and n can be one of the following values: 1/2 for allowed direct, 3/2 for forbidden direct, 2 for allowed indirect, and 3 for forbidden indirect transitions.

In this review, we will keep the terms of energy levels originally used in the publications.

III. PHOTOREACTION

With the aid of light energy, a photoreaction can produce a product that is thermodynamically uphill under dark conditions, such as water splitting and some organic synthesis.³⁵ Typically, photoreaction can be divided into two categories: photochemical reaction and photocatalytic reaction (for organic synthesis, it is generally known as photoredox catalysis; Fig. 2).³⁶ In a photochemical reaction, the reactant itself is prompted to its excited state by absorbing light. The excited state crosses over a small activation energy barrier and forms a product. One of the well-known photochemical reactions is the "electrocyclic reaction," which is a kind of pericyclic rearrangement reaction involved with ring-opening and ring-closing and has been widely applied in fluorescent switching.³⁷ In a photocatalytic reaction, the photocatalyst reaches its excited state by absorbing light. Then, the excited photocatalyst can be either oxidized or reduced by the reactant. These processes sometimes can be assisted with an intermediate such as a redox-shuttle or a co-catalyst. Either way, the reactant is converted to an anion radical, cation radical, or neutral radical that reacts further to the product. For example, several photocatalytic reactions based on

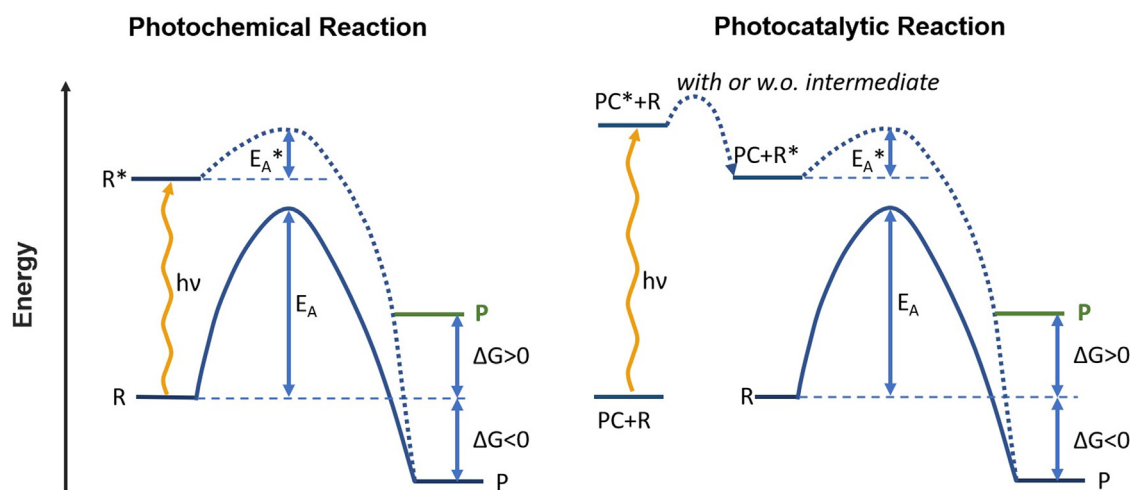


FIG. 2. Two types of typical photoreactions, photochemical reaction, and photocatalytic reaction, R is the ground state of the reactant, R^* is the excited state of the reactant, E_A is the activation energy through the ground state reactant to the product, E_A^* is the activation energy through the excited state reactant to the product, green P is the product which possesses a higher energy level than the reactant, black P is the product which possesses a lower energy level than the reactant, ΔG is the reaction free Gibbs energy.

Eosin Y have been successfully developed.^{38–40} There are several advantages of the photocatalytic reaction compared to the photochemical reaction:

1. By using a light-absorbing photocatalyst, the photoreaction range can be greatly broadened where the reactant needs not be light-absorbing.
2. In presence of a photocatalyst, the reactant can be either oxidized into a cation radical or reduced into an anion radical, which can be modified by tuning the photoredox properties of the photocatalyst.
3. Photochemical reactions normally are achieved under near UV illumination due to the high energy required for a new bond formation. By contrast, the photocatalytic reaction can be extended to almost all the visible spectrum regions up to near-infrared by choosing different photocatalysts based on their optical properties and reaction selectivities.

IV. MECHANISTIC APPROACH FOR PHOTOREDOX CATALYSIS

Typically, the photocatalytic reaction pathway follows one of the two mechanisms depicted in [Scheme 1](#). Generally, in the presence of a light source, the photocatalyst is excited from the ground state to the excited state. This excited state can be quenched either oxidatively or reductively via single electron transfer (SET) in the presence of an electron acceptor (A) or an electron donor (D), respectively.⁴¹ The electron acceptor/donor mentioned here can be either the substrate or a sacrificial reagent.

According to whether the substrates go through net oxidative, net reductive, or redox-neutral transformations, photoredox catalytic processes can be categorized as shown in [Scheme 2](#). A stoichiometric sacrificial oxidant or reducing agent is necessary for net oxidative or net reductive reactions, however in redox neutral reactions, substrates will experience both single electron reduction and oxidation as part of the reaction mechanism.

A. Net oxidative reactions

Net oxidative reactions are the ones in which the substrate is oxidized using photocatalyst by a stoichiometric oxidizing agent.

Net-oxidative transformations rely on a terminal oxidant (sacrificial acceptor of electrons).

B. Net reductive reactions

Net reductive reactions are those in which the substrate is reduced using a photocatalyst by a stoichiometric reducing agent. Net-reductive processes require a terminal reductant (sacrificial source of electrons).

C. Redox neutral reactions

The substrates participate in both phases of the photocatalytic cycle in redox-neutral reactions. For example, the substrate may first constitute the electron donor that reductively quenches the photocatalyst's excited state. The overall reaction becomes redox neutral by re-oxidation of the reduced photocatalyst through an electron uptake of a close-to-product intermediate that is formed during the organic transformation.

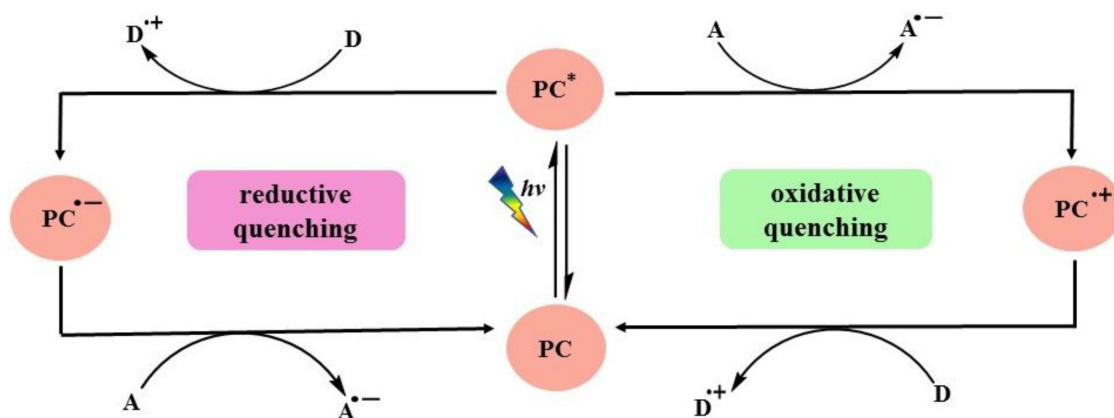
Organic porous materials are having high ability to transform organic reaction under visible light. To comprehend how the light mediated catalytic reaction pathway that a photoredox catalyst may transform the organic product, some spectroscopic techniques, such as ultraviolet-visible (UV-Vis) absorption and emission spectroscopy, spectroelectrochemistry, and transient spectroscopy, are normally used to investigate the reaction kinetics and intermediates. Such mechanistic studies can also offer important insights into the kinetics and intermediates of a reaction and gain knowledge to design new photocatalysts for a photoredox catalytic reaction.

V. ORGANIC POLYMERIC PHOTOCATALYSTS FOR PHOTOREDOX CATALYSIS

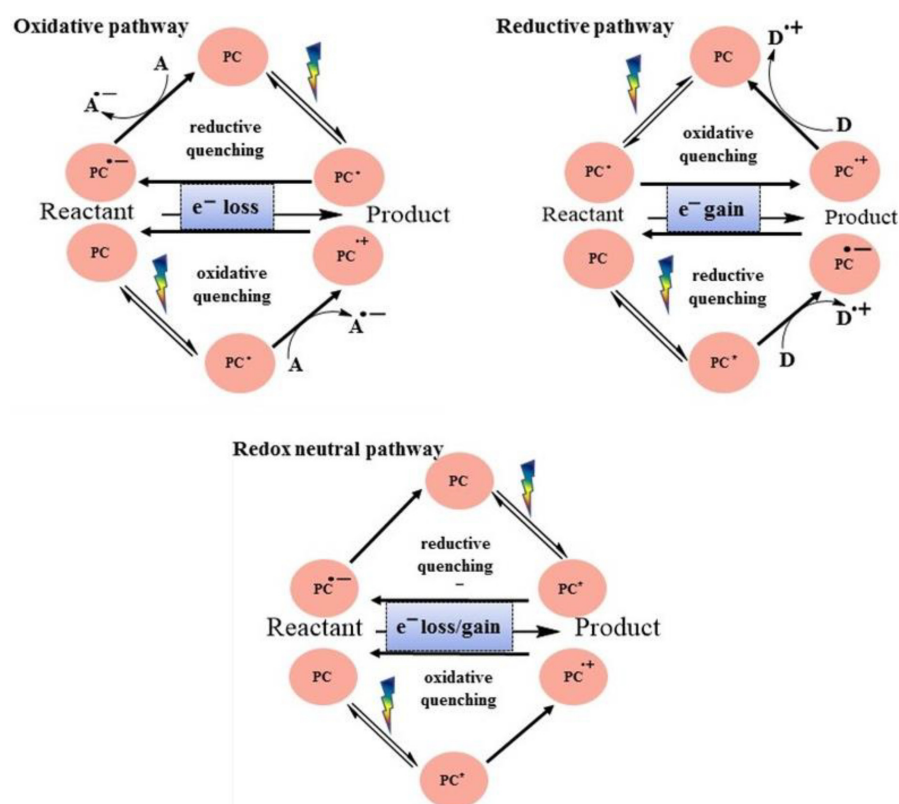
Organic polymeric photocatalysts, such as POP, g-C₃N₄, Cdots, and Pdts, have their advantages and disadvantages. These are summarized in [Table I](#) and thoroughly discussed in Secs. [V A–V F](#).

A. Porous organic polymers (POPs)

POPs ([Scheme 3](#)), which are a more modern type of porous organic material made primarily of organic building blocks joined by



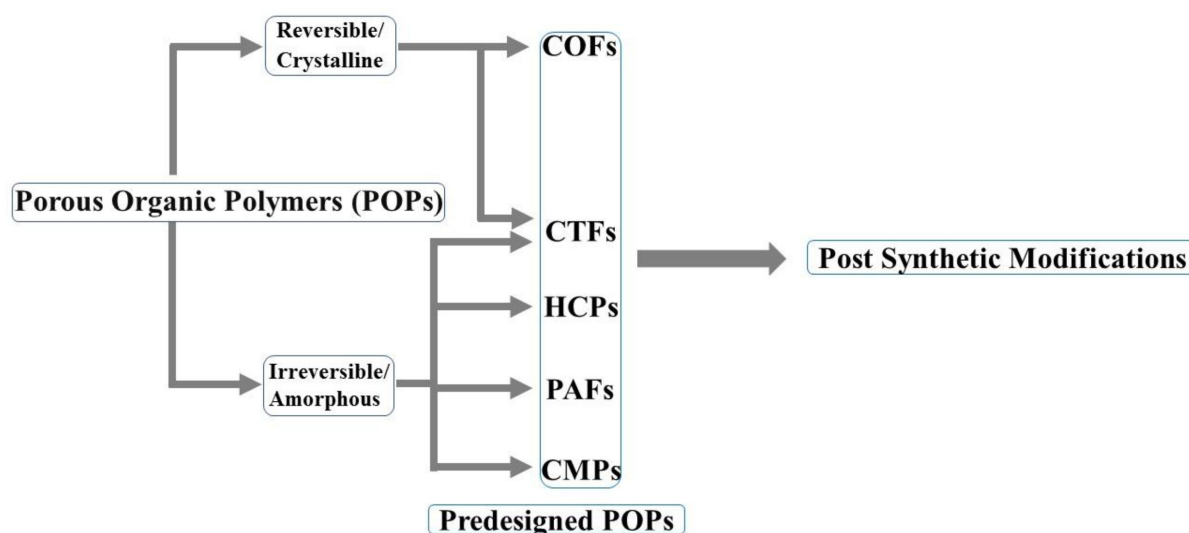
SCHEME 1. Types of quenching pathways in photoredox catalysis, viz., D and A represents electron donor and acceptor that may be substrate/reagent and PC denotes photocatalyst.



SCHEME 2. Net redox events for the visible light-mediated photoredox catalyzed organic transformations.

strong covalent bonds, have recently come into existence. They have stiff, strongly cross-linked frameworks with specific void regions that can accommodate the presence of guest molecules.⁵⁷ Due to their fascinating features, including strong thermal and chemical stabilities, customizable chemical functionalities, huge surface areas, tunable

optical band gaps, and adjustable pore size distributions, POPs have recently gained a lot of study interest as a heterogeneous photocatalyst.⁵⁸ This section provides an overview of existing research examples related to various POPs utilized in photoredox catalysis methodologies while keeping in mind the design principle of possible POP functionality



SCHEME 3. Classification of the porous organic polymers based on the reversible and irreversible nature of the structures.

TABLE I. Comparison chart of the organic polymers.

Types of polymer	POP		Graphitic carbon nitride (g-C ₃ N ₄)	Carbon dots (Cdots)	Polymer dots (Pdots)
	Amorphous POP	Crystalline POP			
Porosity	Mostly microporous broader pore sizes	Micro/Mesoporous narrow PSD (pore size distribution)	Low to high ⁴²	Low ⁴³	—
Crystallinity	Amorphous ⁴⁴	Modest to high	High ⁴⁵	Modest to high ^{46,47}	Low to modest ⁴⁸
Synthetic strategy	Coupling based reaction; sonogashiro based, Schiff base condensation	Self-assembly based on covalent bond imine linkages and triazine linkage	Thermal polymerization, high temperature ⁴⁹	Thermal polymerization, high temperature ^{50,51}	Self-assembly, room temperature ²
Dimensions	Multidimensions	Two or three	Two to three ⁵²	Zero	Zero
Challenges	To have uniform pore size	To increase active sites for catalysis ⁵³	To well control the synthesis, clear relationship between structure and properties ⁵⁴	To well control the synthesis, limited light-harvesting ability ⁵⁵	To prevent aggregation ⁵⁶

adjustment. These POPs are particularly intriguing because they have the potential to be used for photocatalytic oxidation,⁵⁹ reduction,⁶⁰ coupling,^{61,62} and cycloaddition,⁶³ as well as cross dehydrogenative coupling reactions (CDC),^{64,65} C-3 functionalization of indoles,^{66,67} Mannich type reaction.⁵⁷ In terms of structural order, the POPs that have been described so far can be divided into two categories: crystalline and amorphous. While the latter consist of all amorphous POPs, with conjugated microporous polymers (CMPs),^{68–71} hyper-crosslinked polymers (HCPs),^{72–75} polymers of intrinsic microporosity (PIMs),^{76–78} porous aromatic frameworks (PAFs),^{79–81} and amorphous covalent triazine frameworks (CTFs),⁸² the former primarily refers to covalent organic frameworks (COFs)^{83–87} and crystalline covalent triazine frameworks (CTFs).^{88–91}

Over the past decade, there has been much research done on photocatalytic organic transformations using POP-based photocatalysts. This section describes some of representative examples as well as categorizes and summarizes the photocatalytic reactions in POP based-organic transformations. Most of the reactions discussed concern oxidation, reduction, and coupling reactions.

We demonstrate the structural design principles of the POP photocatalysts for a specific application by selecting several examples based on the structure of the pre-synthesized POPs and post-synthetic modification (PSM) into the structure.

The structural design with functionality is a need for producing superior POP-based catalysts by the inherent principle of the catalytic mechanism and the hands-on necessities of heterogeneous photocatalytic systems. For POPs to function as efficient heterogeneous catalysts, it is crucial to take into account the light-harvesting characteristics, tunable optical bandgap, aligned energy levels, easy recyclable property and migration of generated charge, and mass transfer.

B. Design principles

Photocatalysts are brought out of their ground state and into an excited state by absorbing photons. In general, energy, charge, and

atom transfer are the three ways that photoexcited species are involved in the photocatalytic reaction system. The charge transfer of photoexcited species is what initiates most of photoredox organic transformations (as single-electron oxidants or reductants). As a result, it is crucial to determine the redox potential in visible-light-driven processes that include electron transfer to assess the reaction's thermodynamic feasibility. Additionally, it offers the benchmark for choosing and creating appropriate photocatalysts.

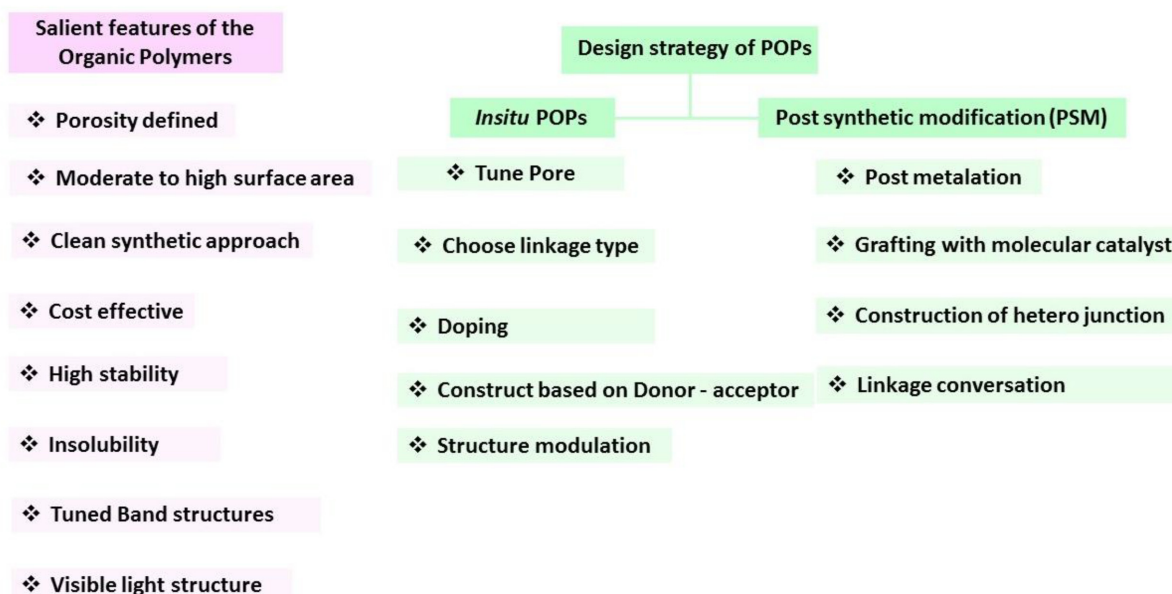
As a crude guideline when designing POP photocatalysts, one needs to

- first check to see if energy levels match the redox potentials of the chemical reactions, i.e., the thermodynamic test that determines whether the reaction can continue.
- Second, for optimum solar energy use with maximum absorption, a suitable energy bandwidth (within the range of 1.7–3.1 eV) within the visible part of the spectrum (400–800 nm) is crucial.
- Third, to achieve high photocatalytic performance, photogenerated charges (holes and electrons) must be successfully separated from one another, and the separated charges must be sufficiently long-lived to carry out the reactions before charge recombination.

When one builds POP-based photocatalysts, one also needs to consider the pore structure qualities and material stability. This is due to the fact that the stability of a catalyst is an inherent prerequisite for accomplishing photoredox catalysis, yet adequate pore diameter and high Brunauer–Emmett–Teller (BET) surface area of the POP photocatalyst typically have a substantial influence on diffusion of the substrate into the matrix of the photocatalyst in order to reach the reactive sites.

C. Design strategy

Several design approaches based on the structure *in situ* (bottom-up) and PSM have been developed, beginning with the design values of POPs as heterogeneous photocatalysts and ultimately aiming for



SCHEME 4. The main characteristics of organic polymers and the design technique for porous organic polymers.

high catalytic efficiency (Scheme 4). While the latter approaches primarily involve linkage conversion, post incorporation of the functional moiety, metal loading, and heterojunction construction, the earlier approaches mainly involve structural variation in the precursor ligands, such as heteroatom doping and metal complexation, and rational design of electron donor–acceptor (D–A) ligands.^{92–94}

The PSM has advantages and disadvantages. Similar to PSM, which has many benefits based on the design of a suitable catalyst with desired properties, such as post-synthetic metalation, incorporation of active catalysts, and metal doping, the challenges include the necessity of an additional synthetic step, uncertainties of where in the material the PSM has occurred, and on whether a sufficient amount of catalyst has been introduced.

1. Oxidation reaction

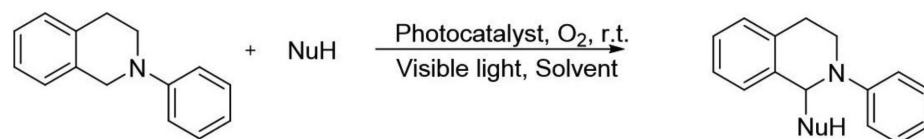
The majority of observed photoredoxcatalytic organic transformations involving POPs are photocatalytic oxidation processes in which superoxide ($O_2^{\cdot-}$) and singlet oxygen (1O_2) are generally the most prevalent reactive oxygen species (ROS). Furthermore, hydroxyl radical ($\cdot OH$) and hydrogen peroxide (H_2O_2) converted directly or indirectly from water or oxygen often play a significant role in the reaction. Plentiful photocatalytic oxidation reactions have been investigated to date, including oxidation of sulfides,⁹⁵ oxidation of benzyl halides,⁹⁶ and oxidative hydroxylation of aryl boronic acids.⁹⁷

a. Photoredox catalyzed cross dehydrogenative coupling reactions. Photoredox-catalyzed cross dehydrogenative coupling (CDC) reactions are prevailing synthetic tools for generating C–C bonds directly and selectively from two different C–H bonds (Scheme 5).

Guo *et al.* recently described *in situ* synthesis of a sequence of hybrid porous polymers (HPPs) [Fig. 3(a)].⁹⁸ This class of polyhedral oligomeric silsesquioxane (POSS), HPP 1–4, was synthesized by a coupling reaction between the OVS and A1, A2, A3, or A4 monomers, as shown in Fig. 3(a). Among the various POPs identified, those based on POSS, a family of silicon-based hybrid molecules, demonstrated particularly good stability as well as exceptional performance as stable heterogeneous catalysts in organic synthesis. These HPPs were successfully used as metal-free heterogeneous photocatalysts for the CDC reaction. The model reaction was the aza-Henry coupling of tetrahydroisoquinolines with nitroalkanes.

The intermediate 1O_2 , formed from 3O_2 sensitization via energy transfer by the excited photocatalyst, was identified by mechanistic investigations [Fig. 3(b)]. In addition to this photocatalytic reaction, good functional group tolerance and recyclability have been achieved. The use of POSS-based luminescent HPPs as photocatalysts in synthetic reactions is demonstrated for the first time in this study.

In a study by Kumar *et al.*, a 2D amide-based porous organic framework (POF) for atom-economic and metal-free visible-light triggered oxidative Mannich reaction was developed as shown in Fig. 4(a).⁹⁹ The C-7 POF was successfully grafted via the solid phase



SCHEME 5. General reaction scheme for the photoredox catalytic CDC reaction.

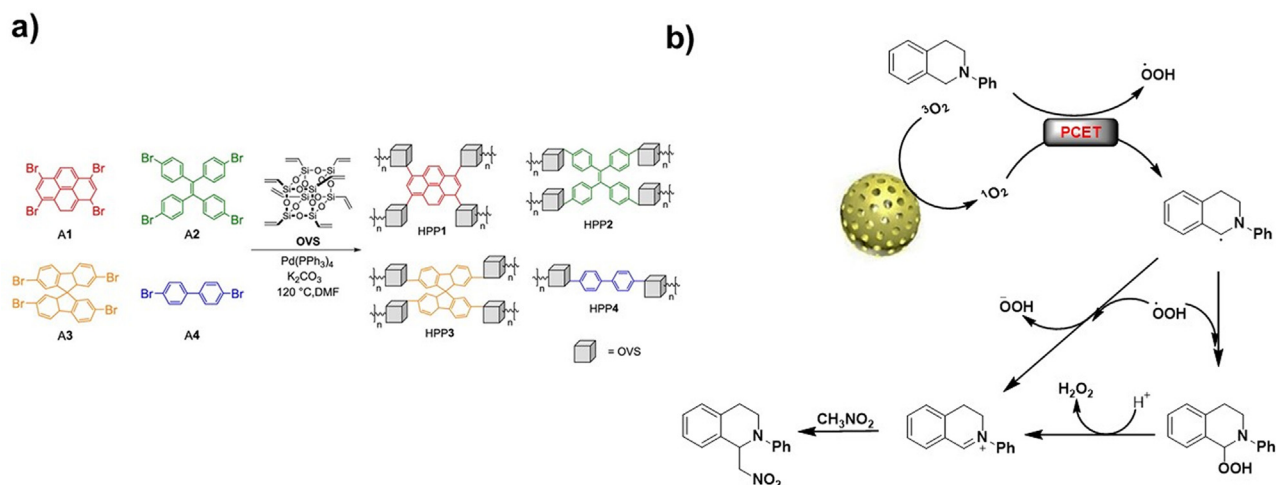


FIG. 3. (a) Synthetic route for POSS-based hybrid porous polymers including chromophores (HPP1–HPP4); (b) proposed catalytic mechanistic approach for the aerobic photo-catalyzed aza-Henry reaction utilizing (HPPs). Reproduced with permission from Guo *et al.*, ACS Appl. Mater. Interfaces **13**, 42889 (2021). Copyright 2021 American Chemical Society.

peptide synthesis (SPPS) with molecular photocatalysts (Rose bengal). It is a successful example of the PSM of the POFs with a bifunctional catalytic group that works synergistically.

Experimental and theoretical shreds of evidence validated the combined photo-organic mechanism as a result of the effective modulation of an energy gap in the catalyst. The atom-economic oxidative Mannich reaction is carried out to the best of the catalytic system, generating the iminium ion intermediate *in situ* [Fig. 4(b)] and

minimizing the number of typical Mannich reaction steps. Similarly, the hooked L-proline moiety with the C-7 POF acts synergistically as a base to catalyze the ketone (2a) to produce enamine (2a'). As a result, nucleophile enamine is added to intermediate (1c) to yield, β -amino ketone (3a).

Zhi *et al.* synthesized three donor–acceptor CMPs via an oxidative coupling reaction. These CMPs based on donor–acceptor (D–A) structures have easily modifiable photoelectric properties and

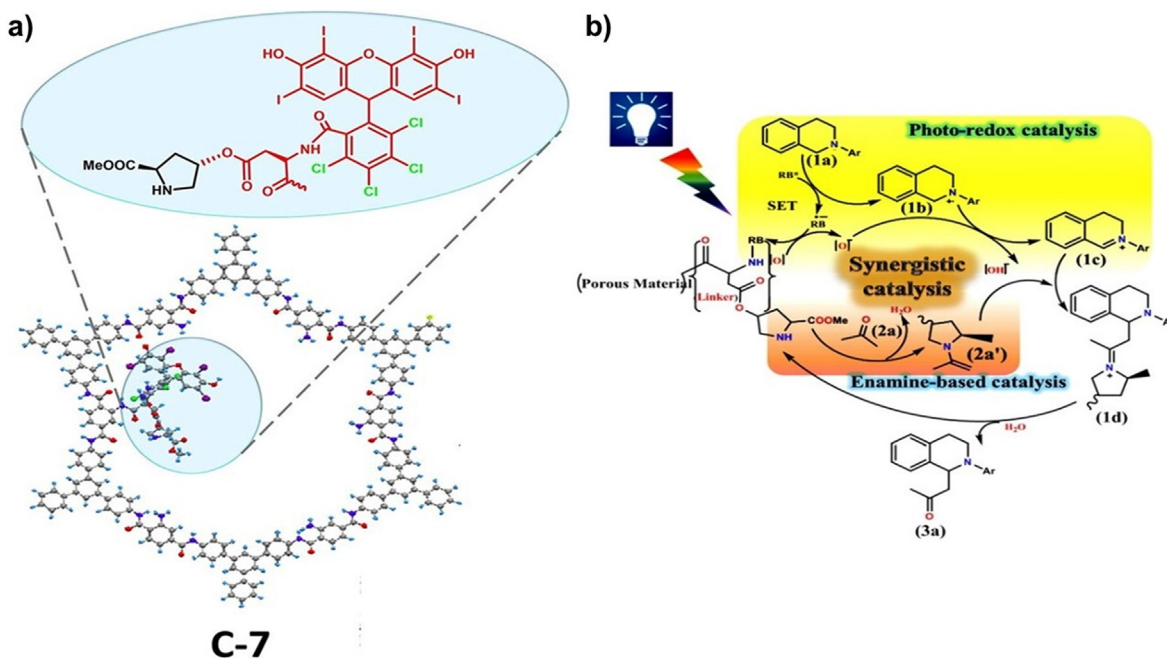


FIG. 4. (a) Representation of dual-catalyst engineered framework C-7; (b) schematic representation for the coupling reaction in between 1a and 2a by bifunctional C-7 photocatalyst. Reproduced with permission from Kumar *et al.*, J. Catal. **394**, 40 (2021). Copyright 2021 Elsevier.

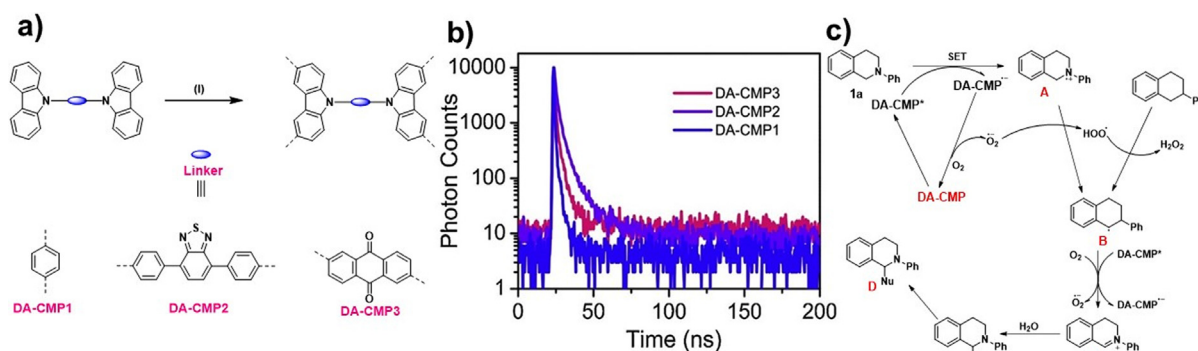
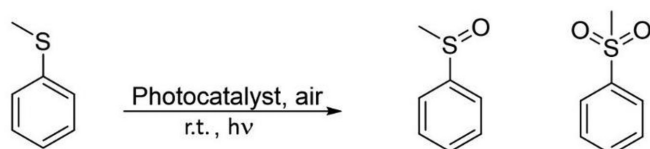


FIG. 5. (a) Synthetic scheme by using FeCl₃/CHCl₃ oxidative coupling polymerization process to create DA-CMPs; (b) Photoluminescence decay traces of DA-CMPs; (c) schematic mechanistic representation for the catalytic C–H functionalization by the DA-CMP photocatalyst. Reproduced with permission from Zhi *et al.*, Appl. Catal., B **244**, 36 (2019). Copyright 2019 Elsevier.



SCHEME 6. General reaction scheme for photocatalytic oxidation of sulfides.

enhanced photocatalytic performance.¹⁰⁰ Figure 5(a) shows how to make these three D-A types of photocatalysts with carbazole and varied units of electron acceptors units.

DA-CMP2 exhibited superior interfacial separation of photo-induced electron–hole pairs and faster charge transport. In addition, the DA-CMP2 lifetime shows a duration of 3.35 ns in Fig. 5(b). The extended lifetime of charge carriers increases their reactivity. Additionally, a proposed catalytic mechanism is provided to explain

the role of the photocatalyst in Fig. 5(c). The final product is produced through a nucleophilic addition reaction after the photocatalyst produces the excited species DA-CMP*, which is then reductively quenched with the substrate 1a via a SET pathway to form cationic A and anionic DA-CMP radicals.

b. Sulfide oxidation. Sulfoxides play an important role in organic synthesis and the pharmaceutical industry as intermediates or biologically active compounds. It is the most effective and atom-economic ways to produce sulfoxides is done by photocatalytic oxidation process of sulfides, which abides by the standards of green synthetic chemistry (Scheme 6).

The incorporation of pure organic dyes, i.e., boranil dye into the backbone of conjugated microporous polymers (CMPs) by Gong *et al.* in 2021 paves the way for the use of molecular photocatalysts in POPs as shown in Fig. 6(a).¹⁰¹ When compared to its boranil-free equivalent, it demonstrated improved photocatalytic performance for the aerobic

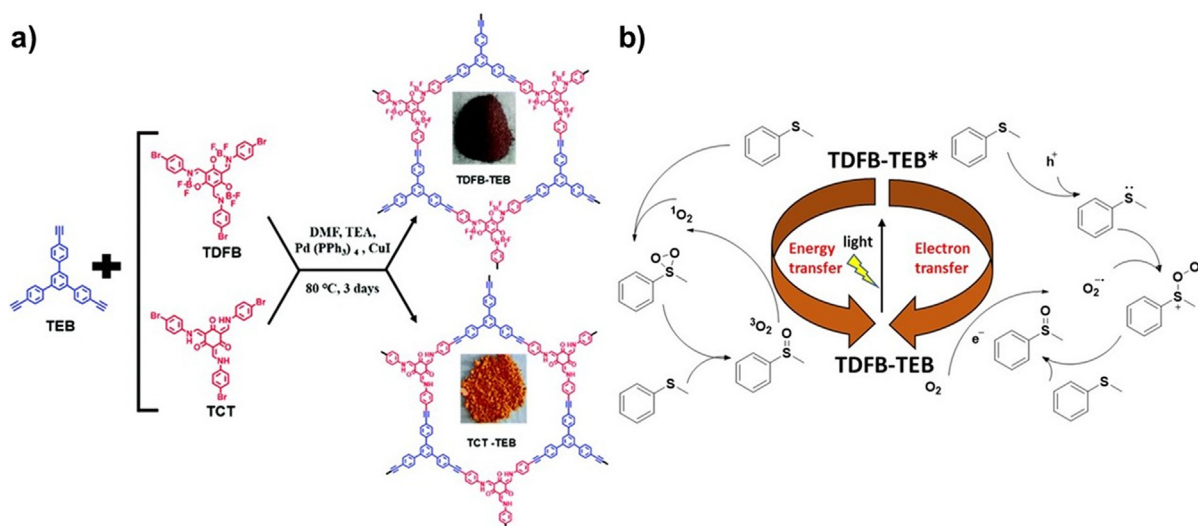


FIG. 6. (a) Synthetic route for the synthesis of conjugated microporous polymers TDFB-TEB and TCT-TEB; (b) proposed reaction mechanism of sulfide using TDFB-TEB as a photocatalyst. Reproduced with permission from Gong *et al.*, Polym. Chem. **12**, 3153 (2021). Copyright 2021 The Royal Society of Chemistry.

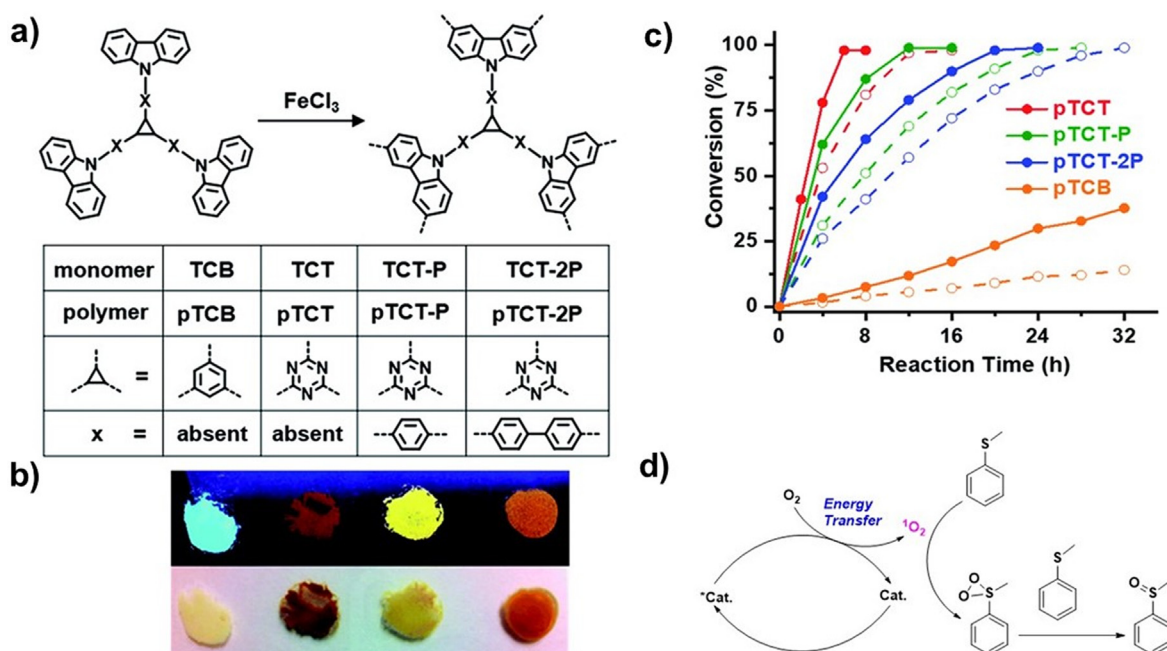


FIG. 7. (a) Synthetic route and chemical structures of the polymers, (b) inset images of POFs in the presence of UV and visible light, (c) conversion chart of reactant to product in CH₃OH (open circle) and CD₃OD (solid circle), and (d) plausible mechanistic approach for the oxidation reaction of sulfides. Reproduced with permission from Luo *et al.*, J. Mater. Chem. A **6**, 15154 (2018). Copyright 2018 The Royal Society of Chemistry.

oxidation of amines and sulfides. Boron complexation increased the visible-light absorption, optical bandgap, and planar conjugation of the material. That is a good example of the design of photocatalysts with enhanced optical properties.

A series of trapping experiments were conducted to better understand the reaction mechanism of the selective oxidation of sulfides to sulfoxides. When compared to its boranil-free equivalent, it demonstrated improved photocatalytic performance for the aerobic oxidation of amines and sulfides. Boron complexation increased the visible-light absorption, optical bandgap, and planar conjugation of the material. Like NaN₃ scavenges ¹O₂ and benzoquinone scavenges O₂^{•−}; both reduce the yield of the products. These results demonstrated the importance of ¹O₂ and O₂^{•−} as active species. Based on the experimental screening results mentioned, plausible reaction pathways for photo-catalytic oxidation of sulfides have been proposed in Fig. 6(b).

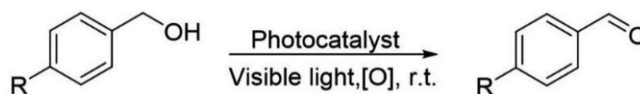
On the other hand, Luo *et al.* reported a class of carbazole-triazine-based (D-A) POFs in a separate method [see Figs. 7(a) and 7(b)].¹⁰² The sequential outline of donor and acceptor units into POFs stabilized the charge-transfer state and permitted an efficient energy transfer to create ¹O₂. Meanwhile, appropriate adjustment of the D-A distance resulted in appropriate photoredox characteristics with results, therefore increasing the efficiency of ROSs formation.

Several experiments suggested that the ¹O₂ pathway is used for sulfide oxidation to sulfoxide. When 2.0 equiv. of NaN₃ (quencher reagent) was used, and no product formation was observed. Addition of well-known O₂^{•−} trapping agent quinone did not affect the process. When performed in CD₃OD, the reaction was greatly accelerated for all POFs due to the prolonged lifetime of ¹O₂ in the deuterated solvent.

The formation of sulfoxide occurs collectively via the ¹O₂ oxidation pathway shown in Fig. 7(c), contrary to the O₂^{•−} mechanism proposed by Loh and colleagues.¹⁰³ In addition, their findings indicated that ¹O₂ is more vigorous than O₂^{•−} for the oxidation process as shown in Fig. 7(d). The stabilized charge separation triplet state could enhance the high photosensitization efficiency of D-A POFs. The addition of N atoms to the triazine core allows for charge transfer and ISC, resulting in triplet excited state stabilization.

c. Oxidations of alcohol. In organic synthesis, the oxidation of alcohols to ketones frequently requires harsh conditions, which warrants the development of new methodologies based on photoredox catalysis (Scheme 7).

At ambient temperature conditions, Huang *et al.* used a thiophene-based triazine framework as an active photocatalyst for the oxidation of alcohols.¹⁰⁴ It was possible to generate a very positive HOMO level at +1.75 V against SCE (standard calomel electrode) by inserting thiophene units into the CTF backbone, resulting in a strong photo-oxidation potential. Furthermore, mesoporous silica was used as a support during the photocatalytic process to clarify the morphological effect and expand the active area of CTF-Th. The framework



SCHEME 7. General reaction scheme for photocatalytic oxidation of alcohols.

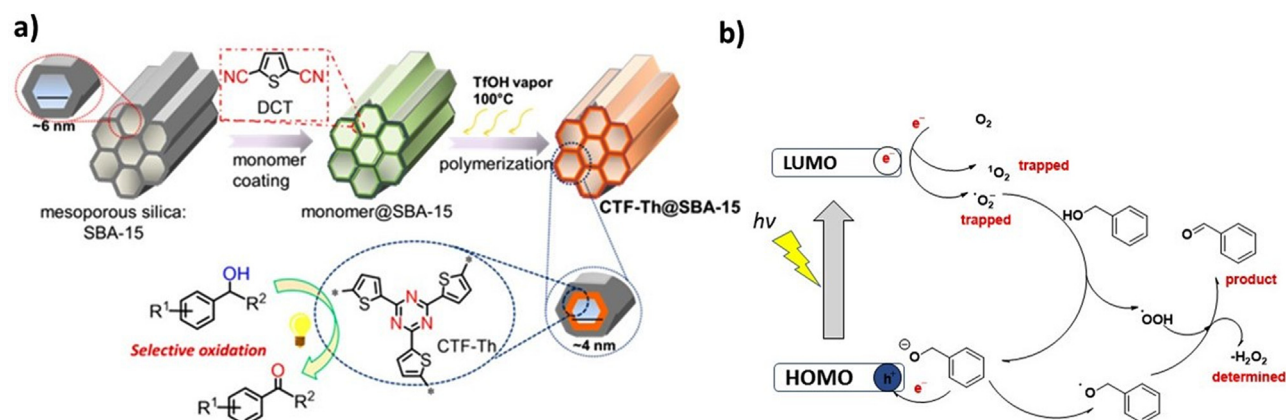
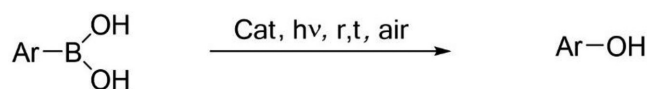


FIG. 8. (a) General synthesis method for thiophene-based CTF-Th on SBA-15; (b) Mechanistic diagram for the photocatalyst's selective oxidation of alcohols. Reproduced with permission from Huang *et al.*, ACS Catalysis 7, 5438 (2017). Copyright 2017 the American Chemical Society.



SCHEME 8. General reaction scheme for photocatalytic oxidative hydroxylation of arylboronic acids.

was directly manufactured onto mesoporous silica (SBA-15) by cyclization polymerization, providing an insoluble yellow powder for the CTF-Th@SBA-15 mesoporous nanoreactor.

The activated forms ($O_2^{\cdot-}$ and 1O_2), are produced from activated O_2 by using the photo-generated electrons, that extract one proton from benzyl alcohol into its anionic form and resulting in the production of $^{\cdot}OOH$ species. In Fig. 8(b), the photogenerated hole first oxidizes the benzyl anion to form an anionic radical, which is then oxidized by $^{\cdot}OOH$ to form benzaldehyde.

d. Oxidative hydroxylation of arylboronic acids. The photocatalytic oxidative hydroxylation of arylboronic acids yields the corresponding phenols in an environmentally friendly and efficient manner as shown in Scheme 8.¹⁰⁵

Luo *et al.* reported a porous organic framework, Cz-POF-1, Fig. 9(a) toward three classical synthetic transformation reactions: dehalogenation, hydroxylation α -alkylation.¹⁰⁶ The hydroxylation reaction undergoes the oxidative quenching pathway because the reduction potential of Cz-POF-1 [$E_{1/2}^{red} = -1.53$ V vs the saturated calomel electrode (SCE)] is proficient in reducing molecular oxygen ($E_{1/2}^{red} = -0.86$ V vs SCE in DMF) to the significant radical species $O_2^{\cdot-}$. Generally, $O_2^{\cdot-}$ is supposed to be active to react with boron via the vacant orbital of the acidic boron.¹⁰⁷ Proton abstraction and aryl shift are carried through to the final product [see Fig. 9(b)]. Cz-POF-1 conjugation properties boost its visible light absorption and accelerate the reaction pace. Because of their potent electron-donating capabilities, the three photoreactions are valuable and catalyzed.

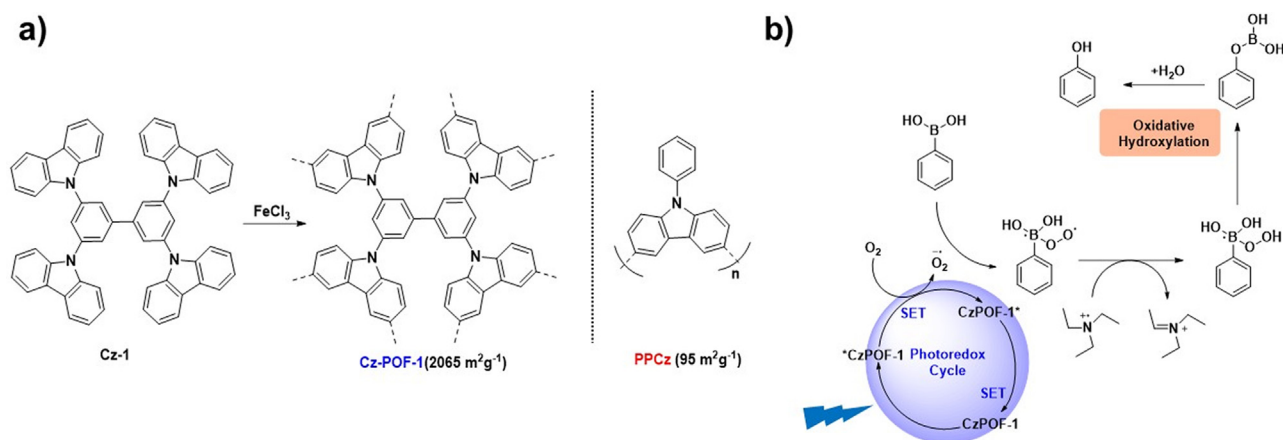


FIG. 9. (a) Synthesis of the porous framework; (b) proposed catalytic mechanism. Reproduced with permission from Luo *et al.*, ACS Catal. 5, 2250 (2015). Copyright 2015 the American Chemical Society.

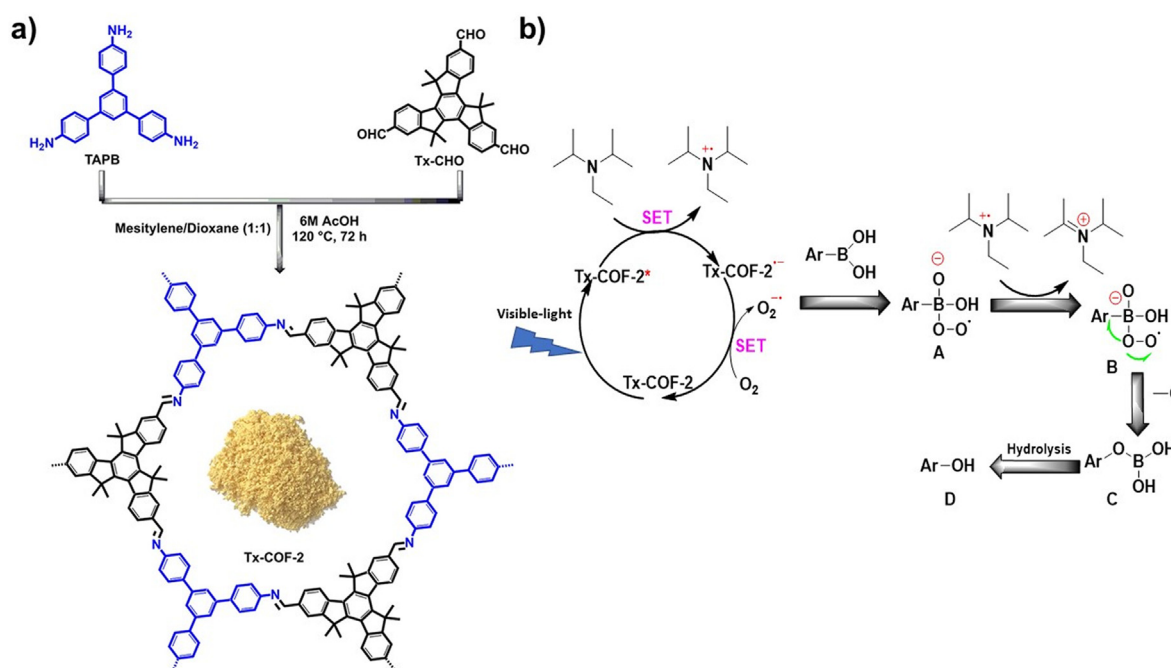


FIG. 10. (a) Synthetic procedure of Tx-COF-2; (b) schematic mechanistic scheme for aryl boronic acids to phenols by a photocatalyst. Reproduced with permission from Nailwal *et al.*, *Macromolecules* **54**, 6595 (2021). Copyright 2021 the American Chemical Society.

Moreover, Nailwal *et al.* synthesized a truxene-based porous framework via a base-catalyzed condensation reaction as shown in Fig. 10(a).¹⁰⁸ Various electronic features of the framework were studied to gain a deeper understanding of the photocatalytic procedure. A plausible reaction mechanism for the transformation is described in Fig. 10(b). Initially, visible light irradiation generated an excited

intermediate, followed by electron extraction from DIPEA via the SET pathway to generate the desired phenolic product D.

In addition, Cheng *et al.* reported the synthesis of two sp^2 C-COFs based on triphenylamine (TPA) donors which could generate persistent radical cations in the presence of oxygen and light [Fig. 11(a)].¹⁰⁹ The originated radical cations are located at the TPA

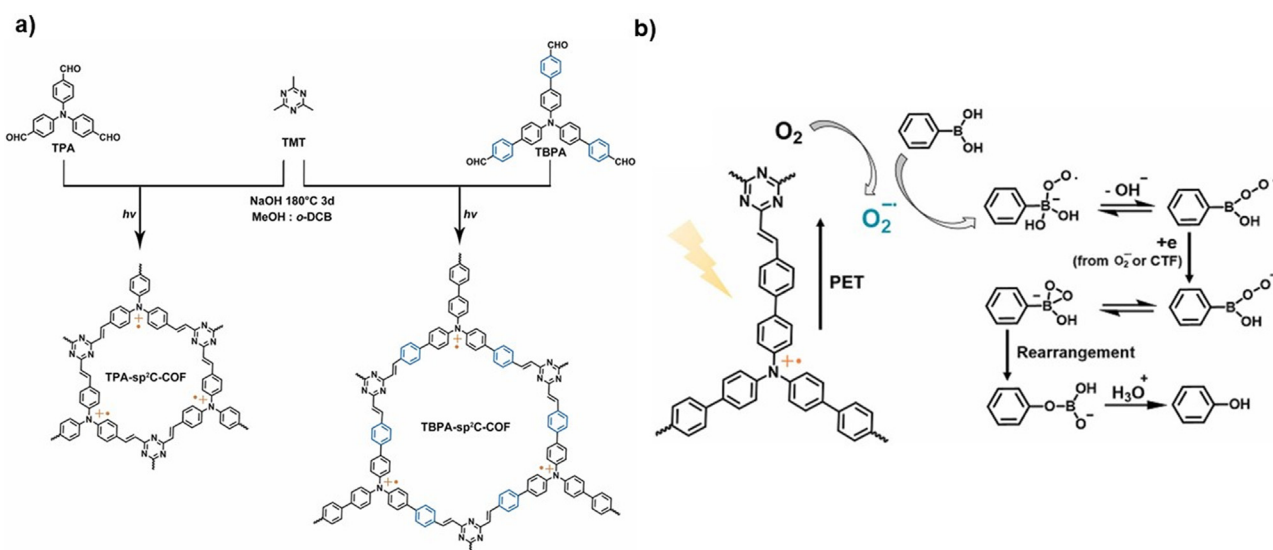
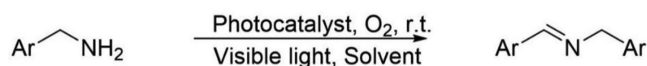


FIG. 11. (a) Synthesis of the radical polymer sp^2 C-COFs via condensation reaction; (b) proposed reaction mechanism of aryl boronic acid oxidative hydroxylation. Reproduced with permission from Cheng *et al.*, *Appl. Catal., B* **306**, 121110 (2022). Copyright 2022 Elsevier.



SCHEME 9. General reaction scheme for the photocatalytic coupling reaction.

units after electron transfer from the excited COF to molecular oxygen. The molecular oxygen finally forms $\text{O}_2^{\bullet-}$. The fs-TA experimental confirmed that the introduction of benzene rings could significantly prolong the lifetime of excited TBPA-sp²C-COF as compared to TPA-sp²C-COF by suppressing the charge recombination between electron donor TPA and acceptor triazine. The long-lived excited state of TBPA-sp²C-COF is responsible for the higher catalytic performance than TPA-sp²C-COF. TBPA-sp²C-COF was, therefore, found to efficiently catalyze the aryl boronic acid oxidative hydroxylation process by efficiently generating ROS [Fig. 11(b)].

2. Coupling reactions

In line with the need for sustainability, the photocatalytic C–C or C–N coupling process by POPs forgoes the widespread use of homogeneous catalysts, especially noble-metal catalysts (Scheme 9). The most significant coupling reaction instances to date are discussed in this section.

Oxidation of benzylamine to imine is also an important reaction to study due to its high significance in organic synthesis utilizing photocatalytic heterogeneous reactions, as well as its high yield. The *in situ* incorporation of organic dyes into CMP photocatalysts with customized properties, as shown in Fig. 6(a), is based on a boranil dye that was used as a photocatalyst.¹⁰¹ Compared to its boranil-free equivalent, a better photocatalytic performance for the aerobic oxidation of amines and sulfides was demonstrated. The results of this work show that boranil dyes are useful as building blocks for the creation of novel photocatalysts for the effective oxidation of amines and sulfides.

Wang *et al.* recently reported four heptazine-based POPs in Fig. 12(a).¹¹⁰ The detailed investigation of the photocatalytic oxidation reaction by varying the length of the benzene unit and the electron density of the linker by increasing the length of the rings and electron density of the linker, the electron donation ability is significantly improved, which also reduces the bandgap of the POP material and

improves its electronic interaction with heptazine, thereby simplifying the separation and transfer of photogenerated carriers. Ultimately, POP-4 showed the best photocatalytic benzylamine oxidation performance. The proposed photocatalytic reaction mechanism of POP-4 is illustrated in Fig. 12(b). Photogenerated electrons and holes react with molecular oxygen and the substrate to form $^1\text{O}_2$ or $\text{O}_2^{\bullet-}$ and amine ions. The final product is formed by the reaction of the reacted anion and anion pairs.

3. Porous organic polymer photoisomerization of olefins

Numerous investigations have focused on the catalytic photoisomerization of thermodynamically stable trans-alkene to less stable cis-alkene, which has been effectively accomplished most often under the UV irradiation (Scheme 10).

Bhadra *et al.* created a triazine as well as a keto-functionalized based COF (TpTt) [Fig. 13(a)].¹¹¹ This photoredox COF catalyst exhibits substantial visible light absorption and has been used in the photoisomerization of uphill conversion reaction of trans-stilbene to cis-stilbene via an energy transfer process in the presence of blue light-emitting diodes via an energy transfer process.

The energy states of potential intermediates during the isomerization reaction were calculated as shown in Fig. 13(b). The photocatalyst gets excited from S_0 to S_1 after absorbing light into the visible spectrum. Following ISC, TpTt enters the stable T1 state and interacts with the substrate, transferring energy. Through the energy transfer process, the substrate is changed into its intermediate state, the radical triplet, which is then changed into the final product.

4. Reductions reactions

Photocatalytic reduction reactions are another important visible light mediated organic transformation. In the presence of light, POP-based photosensitizers generate electron and hole in the presence of light, and the electron then directly interacts with the starting molecules to commence the process. The primary photocatalytic reduction reactions are halo ketone reductive dehalogenation, aromatic nitro compound reduction, and selectively hydrogenation of unsaturated double bonds.

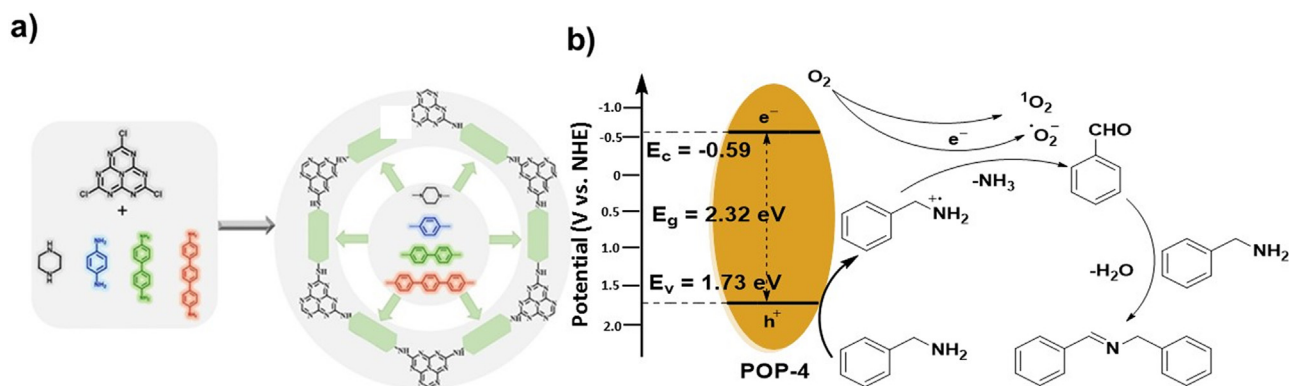
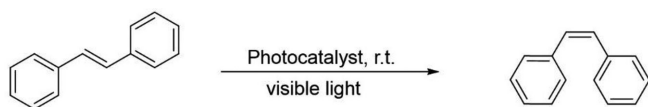
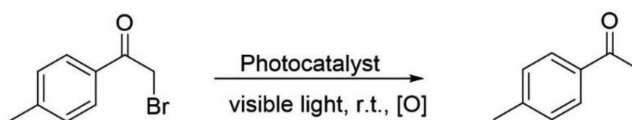


FIG. 12. (a) The general synthetic scheme of heptazine-based POPs; (b) possible mechanism of the oxidation of benzylamine to imines. Reproduced with permission from Wang *et al.*, Chem. Eng. J. **431**, 134051 (2022). Copyright 2022 Elsevier.



SCHEME 10. General reaction scheme for photoisomerization of olefins.



SCHEME 11. General reaction scheme for dehalogenation of halo ketones.

a. Reductive dehalogenation of haloketones. In chemical production processes, dehalogenation is a common and efficient method for converting halogenated hydrocarbons into other compounds as shown in Scheme 11.

A series of the conjugated porous poly-benzobisthiadiazole network were synthesized by Wang *et al.* via high internal phase emulsion polymerization [see Fig. 14(a)].¹¹²

The proposed reaction sequence is depicted in Fig. 14(b). The photo-generated hole in the polymer oxidizes the amine DIPEA and causes the creation of anionic radicals in the polymer. These anionic radicals further react with the substrate, producing the intermediate radical with the departure of the leaving group. The hydrogen donor Hantzsch esters afterwards contribute a hydrogen radical to create the finished product.

b. Reduction of aromatic nitro compounds. Huang *et al.* synthesized a series of nanoporous CTFs (CTF-B and CTF-BT) with a novel triflic acid vapor-assisted solid-phase synthetic approach; triazine frameworks are generally generated in molten ZnCl_2 at high temperatures [Scheme 12 and Fig. 15(a)].¹¹³ These D–A arrangements, such as the BT unit in CTFs, enhance the delocalization of their electrons, tune their band gaps, and expand their absorption range. During the catalytic process, the photoreduction of nitro substrates to amino products involves electron transfer between the CTF-BT and substrate.

Sodium borohydride (NaBH_4) functions both as a source of hydrogen and an electron donor in this context.¹¹⁴

Borohydride was oxidized by the hole generated in the photocatalyst, this was followed with transfer of charge from the photocatalyst's conduction band to the substrate to form its activated intermediate, which extracted hydrogen species from either NaBH_4 or solvent, resulting in the final product.

D. $\text{g-C}_3\text{N}_4$

1. Characteristics of the $\text{g-C}_3\text{N}_4$

Graphitic carbon nitride ($\text{g-C}_3\text{N}_4$) is a kind of organic polymer consisting of sp^2 hybrid carbon and nitrogen atoms. Discovered by Liebig in 1834, and named as C_3N_4 by Franklin in 1922, it did not catch too much attention until 2009 when it was reported as the photo-catalyst for hydrogen production.^{115–117} Since then, research works focusing on $\text{g-C}_3\text{N}_4$ -based photocatalysts have grown rapidly. The synthesis of $\text{g-C}_3\text{N}_4$ involves a high-temperature polymerization process, and defects could be formed during this pyrolysis process as a result of the dynamic problem.¹¹⁸ To a certain extent, these defect sites can act as the active catalytic centers during photo-catalysis reactions, which makes $\text{g-C}_3\text{N}_4$ unique photocatalysts.^{119,120} At the same time, the defects also constitute trap states for charge recombination, which deteriorate the photocatalytic efficiency.¹²¹ One common question in

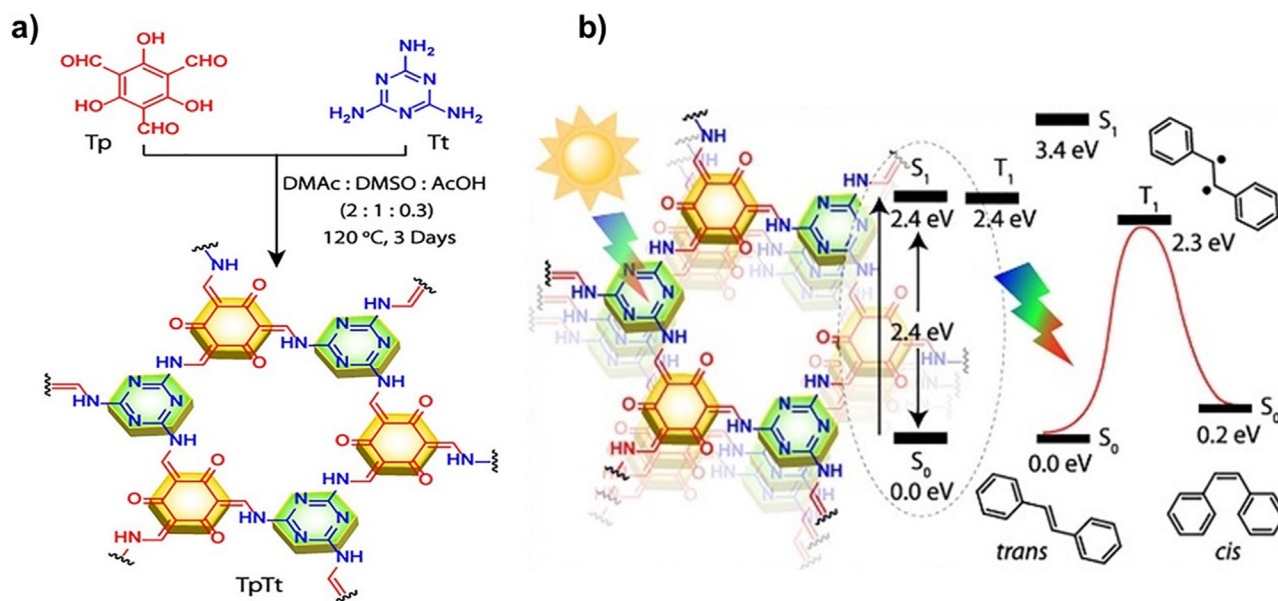


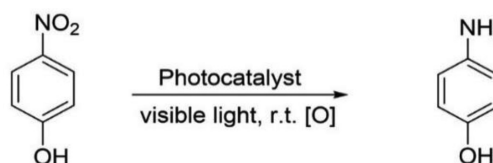
FIG. 13. (a) General synthetic scheme of the TpTt synthesis; (b) using the TpTt COF catalyst, trans to cis photoisomerization of stilbene is shown mechanistically. Reproduced with permission from Bhadra *et al.*, J. Am. Chem. Soc. 141, 6152 (2019). Copyright 2019 the American Chemical Society.

almost all photocatalysis reactions based on g-C₃N₄ is how to keep the balance of this trade-off effect. Modification techniques such as doping, forming the PN heterojunction with other semi-conductors, and morphology engineering, are three of the most widely adopted approaches.¹²² In addition to water splitting,^{123–125} pollutant degradation,^{126,127} and CO₂ reduction,^{128,129} the modified g-C₃N₄ has shown potential to be photoredox catalysts in organic transformation reactions.

2. Oxidation reaction

Inspired by the classical Fenton's reagent, Chen *et al.* developed an iron-doped g-C₃N₄ that could directly oxidize benzene to phenol using hydrogen peroxide, while the undoped material showed no activity.¹³⁰ Density functional theory (DFT) calculations found that g-C₃N₄ can chemically absorb and activate benzene [Fig. 16(a)]. Nevertheless, a doping strategy does not always result in improved photocatalysis reactions. Marci *et al.* found that P-doped and O-doped g-C₃N₄ presented an inferior oxidation catalysis ability, while the thermal-etched group gave a better oxidation yield [Fig. 16(b)]. The reason is that the special surface area of the g-C₃N₄ increased dramatically after the heat treatment, thus giving more space to react with the substrates.^{131,132} The benign effect of morphology engineering was also proved by Su *et al.*, while it was reported that the ultra-thin mesoporous g-C₃N₄ showed a much stronger ability to oxidize alcohol to aldehyde because of its significantly improved surface area [shown in Fig. 16(c)].¹³³

Developing the g-C₃N₄ composite structure with a heterojunction interface is an effective way to accelerate charge separation. Xiao *et al.* found that a binary W₁₈O₄₉/holey ultra-thin g-C₃N₄ nanocomposite prepared via the solvothermal method showed excellent photocatalytic activity for the selective oxidation of benzyl alcohol to benzoic acid with a conversion above 90% in dilute alkaline conditions



SCHEME 12. General reaction scheme for reduction of aromatic nitro compounds.

[Fig. 17(a)].¹³⁴ Following the same principle, Juntrapirom *et al.* designed a g-C₃N₄/BiOBr heterojunction hybrid prepared by a two-step combustion-coprecipitate method. It was found that the oxidative C–N coupling conversion yield of benzylamine reached 94% under the optimal conditions [Fig. 17(c)]. The much-improved catalysis activity was caused by efficient charge transfer and separation originating from a staggered band lineup.¹³⁵ Chai *et al.* discovered that the photo-oxidative coupling of benzylamine based on CeO₂/g-C₃N₄ heterojunction catalyst exhibited a three times faster rate constant compared with the pure CeO₂ or g-C₃N₄ [Fig. 17(d)]. It suggested the formation of heterojunction between the CeO₂ and g-C₃N₄, acting as a channel for the transfer of photo-generated electrons from g-C₃N₄ to CeO₂, which may be partly responsible for the improvement in photo-activity.¹³⁶ Similarly, Samanta *et al.* prepared a BiVO₄/g-C₃N₄ nanocomposite and found that the photo-oxidation yield of aromatic alcohols and amines with O₂ has improved greatly due to their suitable energy level alignment by efficiently transferring the electrons to BiVO₄, leaving a long-lived hole to complete the oxidation reaction [Fig. 17(b)].¹³⁷

3. sp³ C–H activation

Selectively activating sp³ C–H bond is considered to be an efficient synthesis strategy to produce valuable chemicals, such as

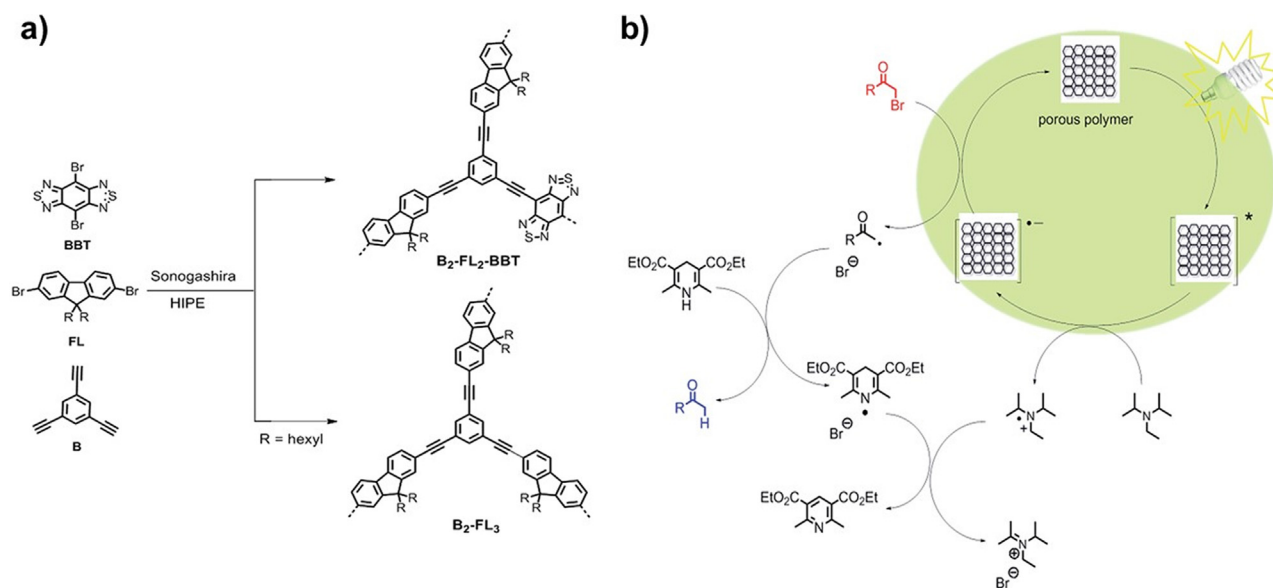


FIG. 14. (a) B₂-FL₂-BBT and B₂-FL₃'s idealized structure and synthetic approach; (b) schematic reaction mechanism for the dehalogenation reaction using the conjugated polymer photocatalysts. Reproduced with permission from Wang *et al.*, J. Mater. Chem. A 2, 18720 (2014). Copyright 2014 The Royal Society of Chemistry.

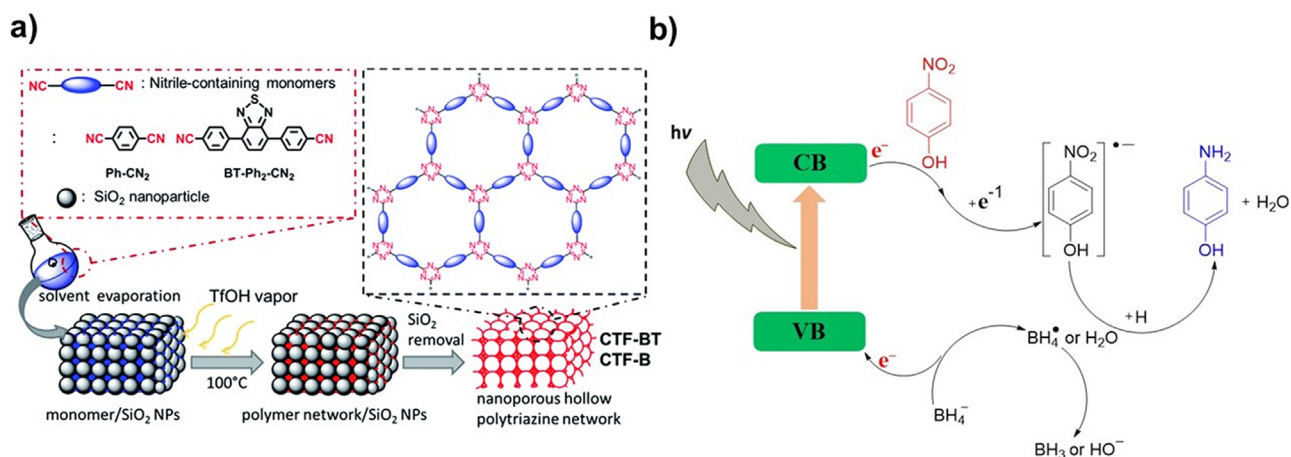


FIG. 15. (a) Solid vapor-phase synthesis is depicted schematically, along with idealized architectures for nanoporous hollow CTFs networks; (b) schematic reaction mechanism for the photoredox catalytic reduction of a substrate to product. Reproduced with permission from Huang *et al.*, *J. Mater. Chem. A* **4**, 7555 (2016). Copyright 2016 The Royal Society of Chemistry.

chemical intermediates and drug molecules. However, sp^3 C–H is a kind of very stable covalent bond, which is stronger than sp^1 C–H and sp^2 C–H. As a result, a great challenge remains to activate this sort of bond. Recently, sp^3 C–H activation with modified C_3N_4 has been

proposed. For example, Qi *et al.* introduced a K^+ -modified C_3N_4 to selectively oxidation of 4-phenyltoluene to corresponding aldehydes with a good conversion yield of 87%, and selectivity of 94% under mild conditions.¹³⁸ In the designed system, C_3N_4 absorbed light and

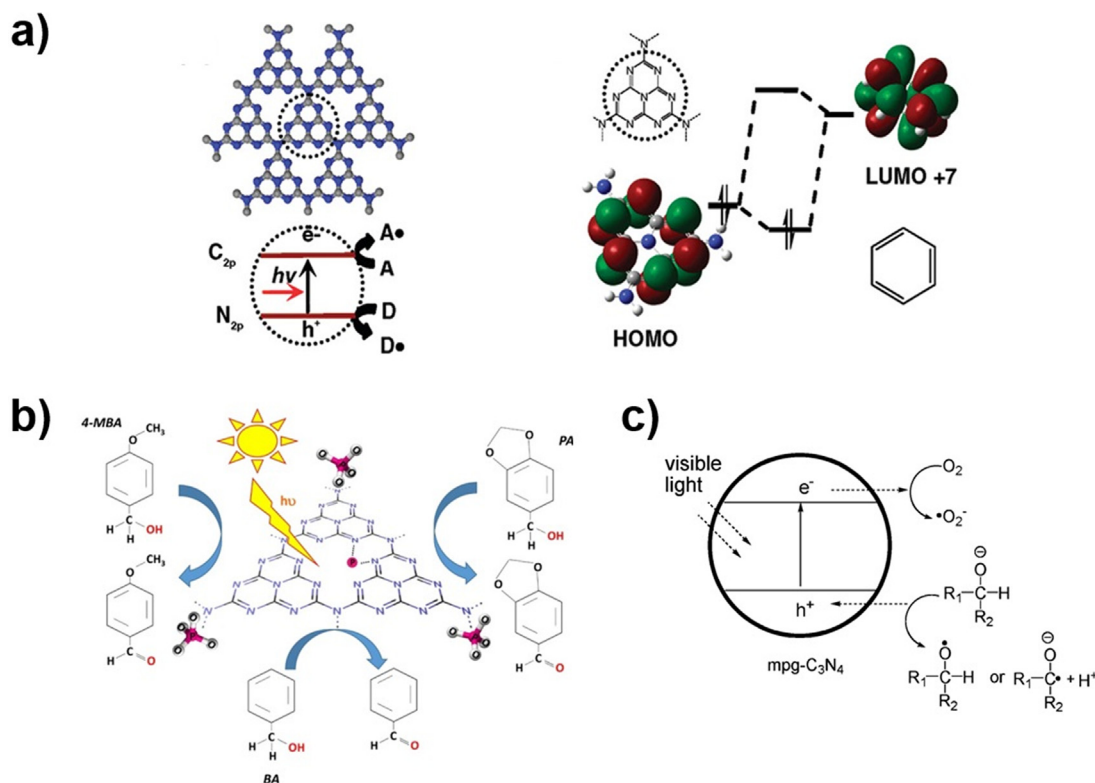


FIG. 16. Scheme of selective photocatalytic oxidation of aromatic alcohols by (a) oxidation of benzene to phenol by Fe-doped $g\text{-C}_3\text{N}_4$; (b) P-doped $g\text{-C}_3\text{N}_4$; (c) C_3N_4 -mesoporous $g\text{-C}_3\text{N}_4$. Reproduced with permission from Chen *et al.*, *J. Am. Chem. Soc.* **131**, 11658 (2009). Copyright 2009 American Chemical Society. Reproduced with permission from Marci *et al.*, *Catal. Today* **328**, 21 (2019). Copyright 2019 Elsevier. Reproduced with permission from Su *et al.*, *J. Am. Chem. Soc.* **132**, 16299 (2010). Copyright 2010 American Chemical Society.

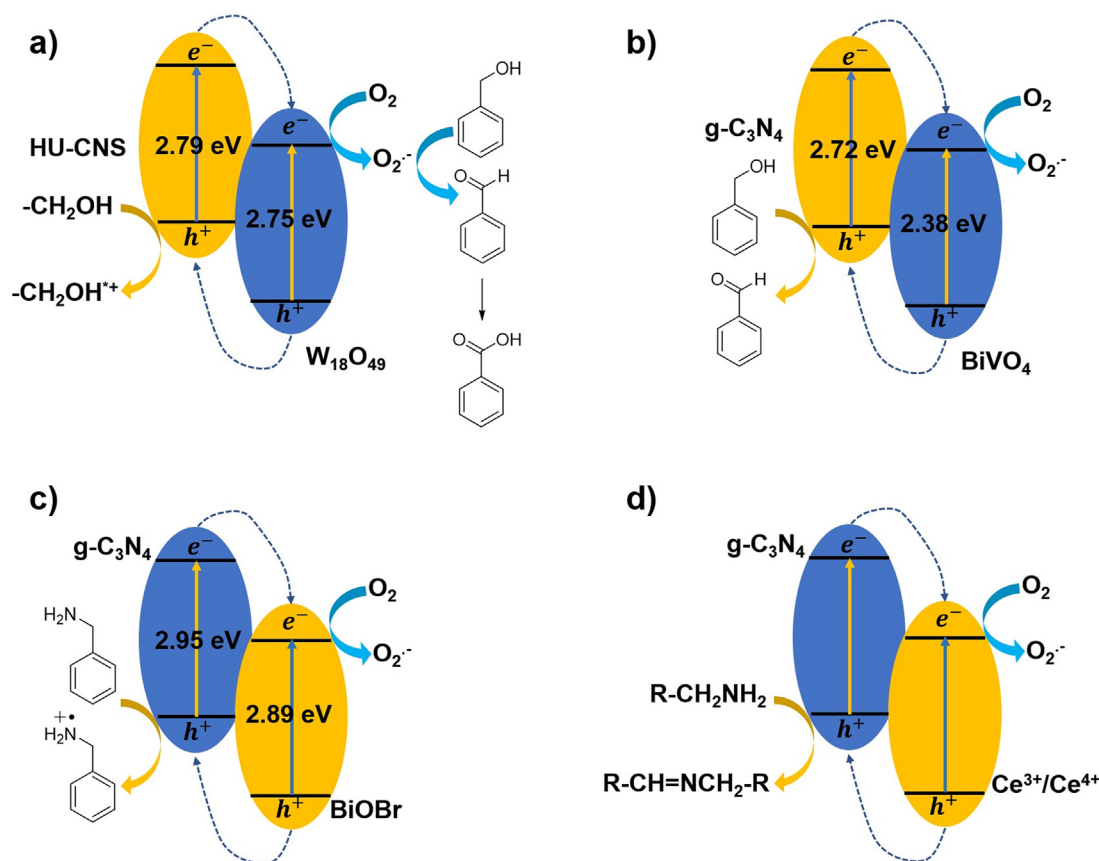


FIG. 17. Forming the PN heterojunction to accelerate the charge separation of (a) g-C₃N₄/W₁₈O₄₉ for benzyl alcohol oxidation; (b) g-C₃N₄/BiVO₄ for oxidation of aromatic alcohols and amines; (c) and (d) g-C₃N₄/BiOBr and g-C₃N₄/CeO₂ for oxidative C–N coupling.^{134–137}

produced tripled excited electrons. After energy transfer from triplet state electron to O₂ to generate O₂¹, which will act as the active species to activate the sp³ C–H bond [Fig. 18(a)]. After being modified with K⁺, this energy transfer process was proved to be efficiently improved.

In addition, Das *et al.* reported a nickel cocatalyst coupled C₃N₄ to directly activate sp³ C–H bond and make the sp³ C–H arylation [Fig. 18(b)].¹³⁹ More than 70 examples have been explored and applied with the proposed method, demonstrating the universality of this

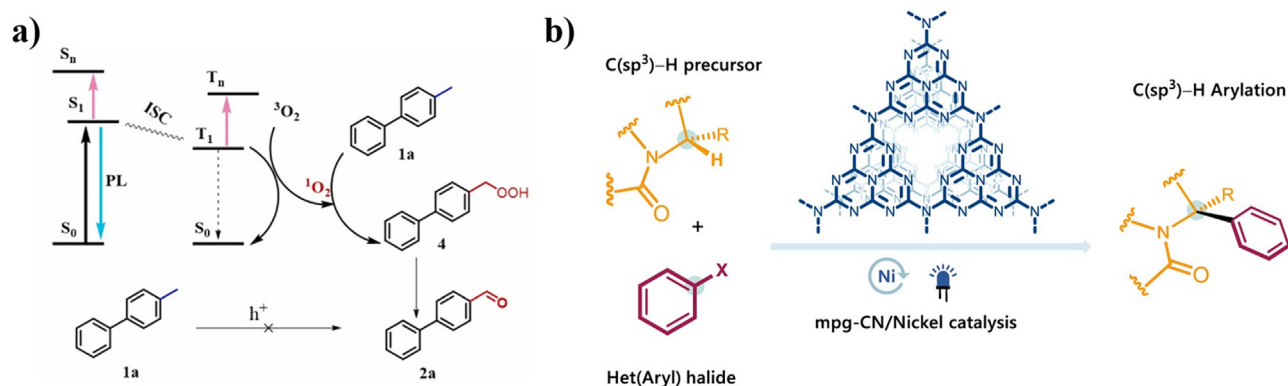


FIG. 18. (a) Alkali metal decorated C₃N₄ for highly selective oxidation of benzyl C(sp³)–H bonds; (b) photocatalytic (Het)arylation of C(sp³)–H bonds with Ni complex modified C₃N₄. Reproduced with permission from Qi *et al.*, Appl. Catal., B 319, 121864 (2022). Copyright 2022 Elsevier. Reproduced with permission from Das *et al.*, ACS Catal. 11, 1593 (2021). Copyright 2022 American Chemical Society.

technique. Control experiments demonstrate that this is a light-driven reaction considering that no obvious product was detected in the absence of light. Mechanistic investigation and kinetic studies suggested that energy transfer from the C_3N_4 to the nickel metal center is the reaction working principle.

sp^3 C–H activation through photocatalysis is still an emerging field with limited examples. Almost all the sp^3 C–H being activated originate from the relatively weak α -H, which could be stabilized due to a certain sort of conjugation after the H radical left. Thus, more explorations are still needed to broaden the university of the sp^3 C–H activation through photocatalysis.

4. Suzuki coupling reaction

Suzuki coupling reaction is one of the most popular C–C bond formation techniques through only one step. The occurrence of Suzuki coupling usually happens under relatively high temperatures to overcome the barrier of carbon–halogen bond breakage. By designing an electron-rich ligand for a Pd catalyst, one can promote the electron transfer from Pd to LUMO of aryl halides and accelerate the rate-determining step. Alternatively, combined with the light-absorbing semiconductor is also a promising way to lower its energy barrier. Li *et al.* for the first time introduced C_3N_4 as the co-catalyst in Suzuki coupling under mild conditions [Fig. 19(a)].¹⁴⁰ The work function of the Pd lies in the bandgap of C_3N_4 , which favors the excited electron transfer from C_3N_4 to Pd upon light illuminating. 16 kinds of substrates have been tested, and excellent reaction yields of aryl iodides with aryl boronic acid under light irradiation at room temperature have been achieved. Recently, Han *et al.* reported a kind of single-atom Cu-doped C_3N_4 used as the co-catalyst for Suzuki coupling [Fig. 19(b)].¹⁴¹ It was found that the charge transfer process from C_3N_4 to Pd could be accelerated due to the electronic effect of CN–Cu, which promotes the electron drifting to the Pd surface, thus benefiting the breakage of the C–I bond. An apparent quantum efficiency of around 19% was obtained under 420 nm light illumination. This study demonstrated that modifying the electronic properties of the supporting material C_3N_4 could regulate photocatalytic activity significantly.

E. Carbon dots

1. Characteristics of carbon dots

Carbon dots (Cdots), also recognized as polymeric carbon dots, are nanometer size objects, typically less than 10 nm, mainly consisting of C, H, and O elements, sometimes containing other elements such as N and S, depending on the preparation method.^{142,143} Cdots usually exhibit excitation-dependent emission from blue light to near-infrared region, which means that the Cdots hold a tunable bandgap due to the quantum confinement effect.¹⁴⁴ These properties make Cdots completely different from pure graphene and graphite, which consist of sp^2 carbon and should have more complex aromatic structures. Due to their high stability, strong luminescence, and flexible bandgap, Cdots have been broadly used in photocatalysis,^{145–147} sensing,^{148–150} bioimaging,^{151,152} and photoredox catalysis.^{153,154}

2. Oxidation reactions

Park *et al.* found that MoS_x -doped Cdots showed greatly improved oxidative C–N coupling photocatalysis activity compared to the individual MoS_x or Cdots. It was proposed that atomic level doping with pyridinic N atoms and MoS_x as well as the special hollow structure was crucial for the significantly improved photocatalytic activity as shown in Fig. 20(a).¹⁵⁵ Similarly, Sarma *et al.* reported sulfated C-dots used as the photocatalyst for aerobic oxidative C–C coupling with a wide range of substrates, including ketones, 1,3-dicarbonyls, and arenes under visible light conditions.¹⁵⁶ Cdots were found to be able to photoactivate the benzylic- CH_2 group in the presence of O_2 by forming the hydroperoxyl intermediate. It demonstrated that surface engineering with the sulfate acid group is favorable to accelerate the catalysis processes by transporting holes to the surface area [Fig. 20(b)]. Modifying the Cdots with a co-catalyst used in traditional organic synthesis during the preparation process is a convenient way to achieve unconventional photoreactions. For example, Cu(I) based complex is an efficient catalyst used in the famous “click reaction.” Consequently, Liu *et al.* developed a zigzag-structured Cu(I)-doped Cdots used in click reaction triggered by UV light without the utilization of reducing agents which is demanded in the traditional

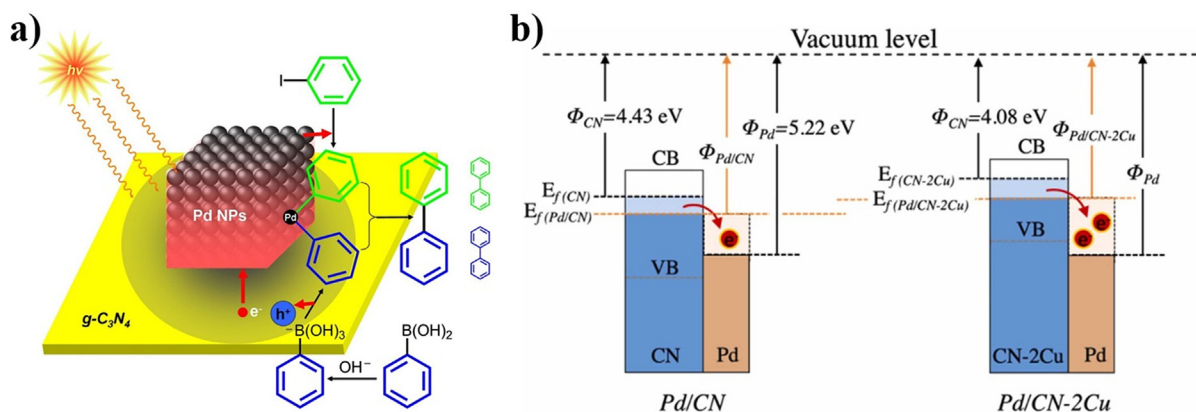


FIG. 19. (a). Scheme of proposed photocatalytic reaction over the C_3N_4 coupled Pd; (b) Schematic illustration of the electron transfer from C_3N_4 to Pd with or without Cu dopant. Reproduced with permission from Li *et al.*, *Sci. Rep.* **3**, 1743 (2013). Copyright 2013 Nature. Reproduced with permission from Han *et al.*, *Appl. Catal.*, B **320**, 121954 (2023). Copyright 2023 Elsevier.

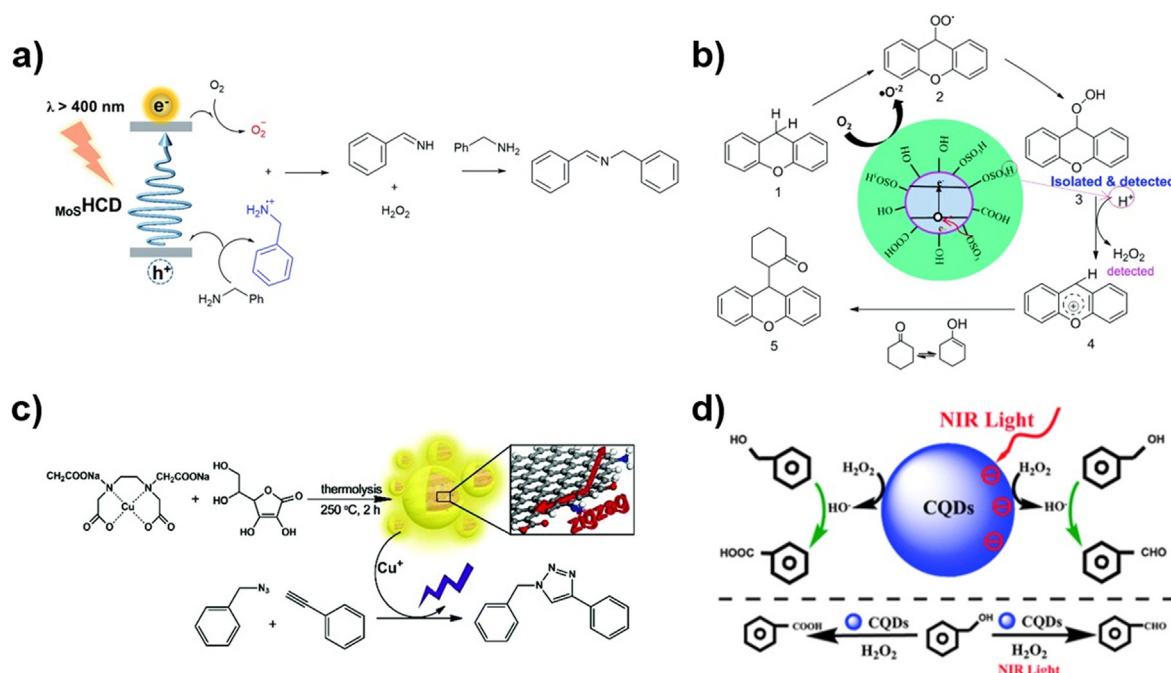


FIG. 20. (a) MoS_x-doped Cdots for photo-oxidative C–N coupling; (b) sulfate acid modified Cdots for photo-oxidative C–C coupling; (c) Cu-doped Cdots for photo-induced click reaction; and (d) light dependent photo-oxidation of benzyl alcohol by Cdots. Reproduced with permission from Park *et al.*, *J. Mater. Chem. A* **4**, 14796 (2016). Copyright 2016 The Royal Society of Chemistry. Reproduced with permission from Sarma *et al.*, *Green Chem.* **21**, 6717 (2019). Copyright 2019 The Royal Society of Chemistry. Reproduced with permission from Liu *et al.*, *Green Chem.* **19**, 1494 (2017). Copyright 2017 The Royal Society of Chemistry. Reproduced with permission from Li *et al.*, *Nanoscale* **5**, 3289 (2013). Copyright 2013 The Royal Society of Chemistry.

reactions. It suggested that electrons initially escaped from the Cdots after forming the photo-excited, leaving holes to repel Cu(I) releasing from the Cdots and catalyzing the reaction [Fig. 20(c)].¹⁵⁷ Oxidizing alcohols to aldehydes or acids selectively in a high yield is of high value in industrial applications. Cdots possess complex bandgap structures, which may exhibit excitation-dependent photocatalysis ability. Li *et al.* discovered that when employed as the photocatalyst, Cdots could selectively oxidize alcohols into aldehydes under infrared light, while oxidizing alcohol into acid under visible light. It suggested that the HO[•] is the main active species responsible for the oxidation reaction [Fig. 20(d)].¹⁵⁸

3. Reduction reactions

There are not many works on photo-reduction reactions employing Cdots as the photocatalyst. It seems that nano-composites with other co-catalysts are widely needed to perform photo-reduction reactions. Chai *et al.* fabricated a Zn-doped CdS/Cdots nano-composite for reducing 4-nitroaniline to p-phenylenediamine in a very short time. As a comparison, the individual Zn-doped CdS or Cdots showed relatively poor photo-reduction ability. It revealed that the C-dots can accelerate the charge separation and transfer efficiency, while Zn doping can adjust the band position of the CdS, thus forming a better energy alignment with the Cdots [shown in Fig. 21(a)].¹⁵⁹ Liu *et al.* developed a type of Pd-doped Cdots/SnS₂ nano-composite and also used it in the photo-reduction of aromatic nitro compounds. Under visible light illumination for 40 min, the conversion rate of 4-

nitrophenol reaches 99.7% using the composite catalyst. Control experiments demonstrated that the as-prepared composite catalyst showed much faster reduction kinetics and good recycling ability. The enhanced catalysis efficiency is attributed to the Cdots promoting the charge carrier separation on SnS₂ and improving the adsorption of active hydrogen from NaBH₄ [shown in Fig. 21(b)].¹⁶⁰

F. Polymer dots

The polymer nanoparticles known as organic polymer dots (Pdts) range in size from 1 to 100 nm.² As a fluorescent probe and reagent to produce active oxygen species for photodynamic treatment, Pdts have been extensively employed in biochemistry.^{24,161} Our group used Pdts for photocatalytic hydrogen production for the first time in 2016 and discovered that Pdts performed five orders of magnitude better than the bulk material.¹⁶² The dimensions of Pdts are much smaller compared to bulk materials, which reduces the distance that photo-generated charges must travel to reach the surface of photocatalyst particles. Heterojunction polymer nanoparticles have been developed recently to further enhance the charge separation within the particle and improve photocatalysis for hydrogen production.^{163–165}

We recently developed a binary Pdts photocatalyst consisting of 1-[3-(methoxycarbonyl)propyl]-1-phenyl-[6,6]C61 (PCBM) as electron acceptor and poly(9,9-dioctylfluorene-alt-benzothiadiazole) (PFBT) as electron donor [shown in Fig. 22(a)].¹⁶⁶ The PFBT/PCBM binary Pdts as a photocatalyst can generate up to 188 mmol of H₂O₂ per gram per hour under alkaline conditions (1 M KOH). At 450 nm,

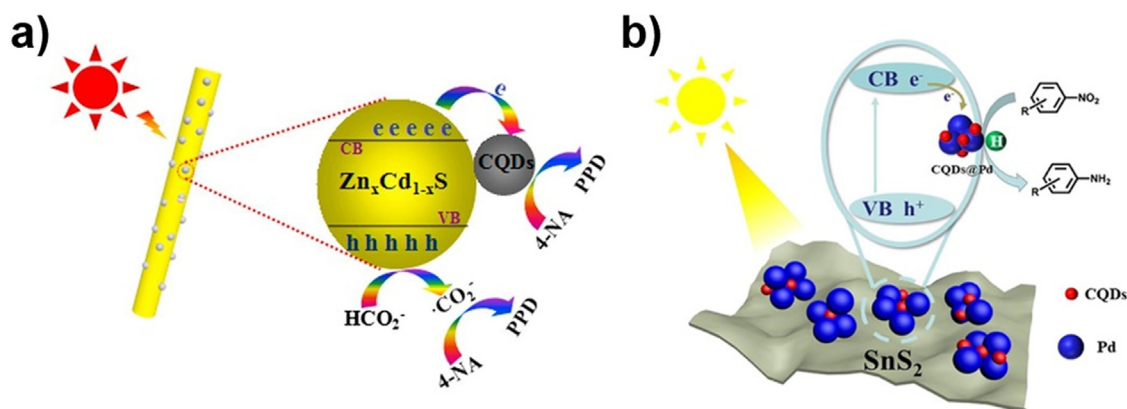


FIG. 21. Scheme of photo-reduction aromatic nitro compounds based on (a) Zn-doped CdS/CdS nano-composite; (b) Pd-doped CdS/SnS₂ nano-composite. Reproduced with permission from Chai *et al.*, *Appl. Surface Sci.* **450**, 1 (2018). Copyright 2018 Elsevier. Reproduced with permission from Liu *et al.*, *J. Colloid Interface Sci.* **555**, 423 (2019). Copyright 2019 Elsevier.

the external quantum efficiencies (EQE) reached to 30% after 5 min and 14% after 75 min. For oxidation reaction, PFBT/PCBM Pdots carried out photooxidation of methanol. Consequently, a thorough photocatalytic reaction procedure is suggested in Fig. 22(b). It was proposed that formate and H₂O₂ are produced in a 1:1 ratio through two possible potential paths: disproportionation reaction and an oxidation reaction. Green organic synthesis using Pdots will be an appealing strategy in the future due to the fact that Pdots are well dispersed in water and have good photophysical properties to perform photocatalysis.

VI. PERSPECTIVE

In summary, photoredox catalysis offers appealing alternatives to traditional thermal reaction methodologies as a lot of the energy input to drive the reactions is provided by light illumination. Among the variety of photocatalysts, organic polymers have drawn great attention due to their large amount of available building blocks, feasible synthesis methods, conveniently tunable physical and chemical properties, excellent intra-molecular charge transport ability, and intrinsic stability. By constructing complex supermolecular configuration and morphology via repeating simple cross-linking organic reactions, a high

specific surface area can be obtained, such as in POPs and C₃N₄. A higher exposed specific surface area of the catalyst means a higher chance to react with the substrate, thus improving the catalysis efficiency. However, the specific surface area cannot be increased indefinitely, as mass transport would then become the overall limiting factor during the photoredox catalysis reactions.

The range at which light is absorbed by the photocatalyst may be another trade-off issue. Broadening the absorption range of the photoredox catalyst means a more efficient usage of the solar spectrum. However, the reaction still requires a certain driving force, and a too small bandgap of the catalyst may provide sufficient energy and become limiting. In addition to absorbing light, the active reaction site is another point that needs to be considered. Incorporating the heterocyclic aromatic compounds into the polymer blocks is an effective technique to fabricate effective photocatalysts as they usually show excellent catalytic activity, without being transition metal-based complexes. To construct a “host-guest” system is a newly emerging approach used in designing COF photocatalysts.

Efficiently separating and transporting the photogenerated charges is essential to the high-efficient photoredox catalysis reactions. Rationally designed D–A molecular structures are commonly adopted

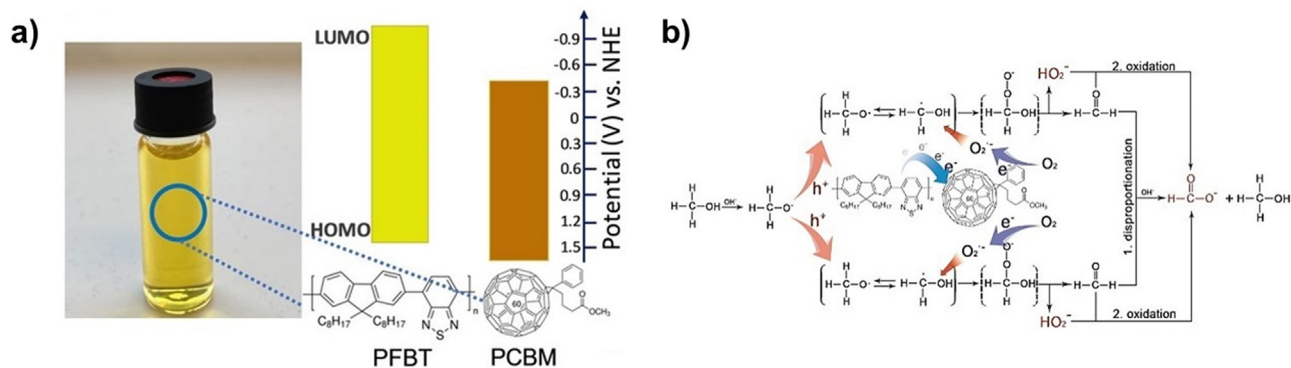


FIG. 22. (a) Energy level profiles and structures of donor and acceptor and the picture of a D–A Pdots solution; (b) The proposed catalytic H₂O₂ and formate production with D–A binary Pdots. Reproduced with permission from Wang *et al.*, *Angew. Chem. Int. Ed.* **61**(23), e202202733 (2022). Copyright 2022 Wiley.

approaches to accelerate the charge separation within the molecule. Blending several kinds of material to compose the PN junction is worth to be considered, among which, heterojunction Pdots are an excellent form to perform this approach.

Although many photoredox catalysis reactions based on polymer catalysts have been successfully performed, constructing low-cost, high-efficiency, and stable polymer catalysts remains a challenge. More attention in the future should be given to the specific properties of the different polymeric photocatalysts such as POP, C_3N_4 , Cdots, and Pdots when coming to their applications in various fields. For example, POP materials might be more suitable for small-molecules-related catalysis involving gaseous products because of their high porosity. Cdots and Pdots can be homogeneously dispersed in water, exhibiting the potential of adjustable surface modification, which could preferentially be utilized in future green organic synthesis. As the absorption range of C_3N_4 is relatively narrow as compared to that of other organic polymers, C_3N_4 could be combined with other light-absorbing photocatalysts or act as a scaffold to enhance photocatalytic performance. The development of new materials and the mechanistic study of their photoredox catalytic reactions will make future reactions more efficient and stable, further paving the way for applications in pharmaceutical industry and biology.

ACKNOWLEDGMENTS

Financial support from the Wallenberg Academy Fellow program from K&A Wallenberg Foundation (Grant No. 2019.0156), a project grant from the Knut and Alice Wallenberg Foundation (Grant No. 2019.0071), and the Wenner-Gren Foundation (Grant No. UPD2021-0151) is gratefully acknowledged.

AUTHOR DECLARATIONS

Conflict of Interest

The authors have no conflicts to disclose.

Author Contributions

Gaurav Kumar and Bin Cai contributed equally to this work.

Gaurav Kumar: Writing – original draft (lead). **Bin Cai:** Writing – original draft (lead). **Sascha Ott:** Funding acquisition (lead); Writing – review & editing (equal). **Haining Tian:** Funding acquisition (lead); Project administration (lead); Supervision (lead); Writing – review & editing (lead).

DATA AVAILABILITY

Data sharing is not applicable to this article as no new data were created or analyzed in this study.

REFERENCES

- Y. Wang, A. Vogel, M. Sachs, R. S. Sprick, L. Wilbraham, S. J. A. Moniz, R. Godin, M. A. Zwiijnenburg, J. R. Durrant, A. I. Cooper, and J. Tang, "Current understanding and challenges of solar-driven hydrogen generation using polymeric photocatalysts," *Nat. Energy* **4**(9), 746–760 (2019).
- M. V. Pavliuk, S. Wrede, A. Liu, A. Brnovic, S. Wang, M. Axelsson, and H. Tian, "Preparation, characterization, evaluation and mechanistic study of organic polymer nano-photocatalysts for solar fuel production," *Chem. Soc. Rev.* **51**(16), 6909–6935 (2022).
- J. Amaro-Gahete, M. V. Pavliuk, H. Tian, D. Esquivel, F. J. Romero-Salguero, and S. Ott, "Catalytic systems mimicking the [FeFe]-hydrogenase active site for visible-light-driven hydrogen production," *Coord. Chem. Rev.* **448**, 214172 (2021).
- S. Mondal, N. S. Powar, R. Paul, H. Kwon, N. Das, B. M. Wong, S.-I. In, and J. Mondal, "Nanoarchitectonics of metal-free porous polyketone as photocatalytic assemblies for artificial photosynthesis," *ACS Appl. Mater. Interfaces* **14**(1), 771–783 (2022).
- A. Saravanana, P. Thamarai, P. S. Kumar, and G. Rangasamy, "Recent advances in polymer composite, extraction, and their application for wastewater treatment: A review," *Chemosphere* **308**, 136368 (2022).
- J. Li, J. Rao, and K. Pu, "Recent progress on semiconducting polymer nanoparticles for molecular imaging and cancer phototherapy," *Biomaterials* **155**, 217–235 (2018).
- X. Sun, S. Jiang, H. Huang, H. Li, B. Jia, and T. Ma, "Solar energy catalysis," *Angew. Chem. Int. Ed.* **2022**, e202204880.
- H. Song, S. Luo, H. Huang, B. Deng, and J. Ye, "Solar-driven hydrogen production: Recent advances, challenges, and future perspectives," *ACS Energy Lett.* **7**(3), 1043–1065 (2022).
- Q. Qi, W. Zhang, and R. Cao, "Solar-to-hydrogen energy conversion based on water splitting," *Adv. Energy Mater.* **8**(5), 1701620 (2018).
- L. Lin, T. Hisatomi, S. Chen, T. Takata, and K. Domen, "Visible-light-driven photocatalytic water splitting: Recent progress and challenges," *Trends Chem.* **2**(9), 813–824 (2020).
- F. Hassanzadeh-Afruzi, "Synergistic photocatalytic effect," in *Heterogeneous Micro and Nanoscale Composites for the Catalysis of Organic Reactions*, edited by A. Maleki (Elsevier, 2022), Chap. 12, pp. 183–195.
- X. Li, J. Yu, and M. Jaroniec, "Hierarchical photocatalysts," *Chem. Soc. Rev.* **45**(9), 2603–2636 (2016).
- M. Antoniadou, V. M. Daskalaki, N. Balis, D. I. Kondarides, C. Kordulis, and P. Lianos, "Photocatalysis and photoelectrocatalysis using (CdS-ZnS)/TiO₂ combined photocatalysts," *Appl. Catal., B* **107**(1), 188–196 (2011).
- J. D. Bell and J. A. Murphy, "Recent advances in visible light-activated radical coupling reactions triggered by (i) ruthenium, (ii) iridium and (iii) organic photoredox agents," *Chem. Soc. Rev.* **50**(17), 9540–9685 (2021).
- C. K. Prier, D. A. Rankic, and D. W. C. MacMillan, "Visible light photoredox catalysis with transition metal complexes: Applications in organic synthesis," *Chem. Rev.* **113**(7), 5322–5363 (2013).
- Y. Kuramochi and O. Ishitani, "Iridium(III) 1-phenylisoquinoline complexes as a photosensitizer for photocatalytic CO₂ reduction: A mixed system with a Re(I) catalyst and a supramolecular photocatalyst," *Inorg. Chem.* **55**(11), 5702–5709 (2016).
- G. Han, G. Li, J. Huang, C. Han, C. Turro, and Y. Sun, "Two-photon-absorbing ruthenium complexes enable near infrared light-driven photocatalysis," *Nat. Commun.* **13**(1), 2288 (2022).
- S. Sharma and A. Sharma, "Recent advances in photocatalytic manipulations of Rose Bengal in organic synthesis," *Org. Biomol. Chem.* **17**(18), 4384–4405 (2019).
- Y. C. Teo, Y. Pan, and C. H. Tan, "Organic dye-photocatalyzed acylnitroso ene reaction," *ChemCatChem* **5**(1), 235–240 (2013).
- S. P. Pitre, C. D. McTiernan, and J. C. Scaiano, "Library of cationic organic dyes for visible-light-driven photoredox transformations," *ACS Omega* **1**(1), 66–76 (2016).
- G.-B. Wang, S. Li, C.-X. Yan, F.-C. Zhu, Q.-Q. Lin, K.-H. Xie, Y. Geng, and Y.-B. Dong, "Covalent organic frameworks: Emerging high-performance platforms for efficient photocatalytic applications," *J. Mater. Chem. A* **8**(15), 6957–6983 (2020).
- H. Wang, H. Wang, Z. Wang, L. Tang, G. Zeng, P. Xu, M. Chen, T. Xiong, C. Zhou, X. Li, D. Huang, Y. Zhu, Z. Wang, and J. Tang, "Covalent organic framework photocatalysts: Structures and applications," *Chem. Soc. Rev.* **49**(12), 4135–4165 (2020).
- T. Zhang, G. Xing, W. Chen, and L. Chen, "Porous organic polymers: A promising platform for efficient photocatalysis," *Mater. Chem. Front.* **4**(2), 332–353 (2020).
- C. Dai and B. Liu, "Conjugated polymers for visible-light-driven photocatalysis," *Energy Environ. Sci.* **13**(1), 24–52 (2020).

- ²⁵A. Savateev and M. Antonietti, "Heterogeneous organocatalysis for photoredox chemistry," *ACS Catal.* **8**(10), 9790–9808 (2018).
- ²⁶J. H. Kim, D. W. Kang, H. Yun, M. Kang, N. Singh, J. S. Kim, and C. S. Hong, "Post-synthetic modifications in porous organic polymers for biomedical and related applications," *Chem. Soc. Rev.* **51**(1), 43–56 (2022).
- ²⁷R. Y. Liu, S. Guo, S.-X. L. Luo, and T. M. Swager, "Solution-processable microporous polymer platform for heterogenization of diverse photoredox catalysts," *Nat. Commun.* **13**(1), 2775 (2022).
- ²⁸D. Frackowiak, "The Jablonski diagram," *J. Photochem. Photobiol. B* **2**(3), 399 (1988).
- ²⁹J. Zhao, K. Xu, W. Yang, Z. Wang, and F. Zhong, "The triplet excited state of Bodipy: Formation, modulation and application," *Chem. Soc. Rev.* **44**(24), 8904–8939 (2015).
- ³⁰B. Liu, X. Zhao, C. Terashima, A. Fujishima, and K. Nakata, "Thermodynamic and kinetic analysis of heterogeneous photocatalysis for semiconductor systems," *Phys. Chem. Chem. Phys.* **16**(19), 8751–8760 (2014).
- ³¹N. Suzuki, "X-ray photoelectron spectroscopy and its application to carbon," in *Carbon Alloys*, E.-I. Yasuda, M. Inagaki, K. Kaneko, M. Endo, A. Oya, and Y. Tanabe (Elsevier Science, Oxford, 2003), Chap. 13, pp. 211–222.
- ³²N. Casado and D. Mecerreyes, "Introduction to redox polymers: Classification, characterization methods and main applications," in *Redox Polymers for Energy and Nanomedicine* (The Royal Society of Chemistry, 2021), Chap. 1, pp. 1–26.
- ³³T. Li, J. Benduhn, Y. Li, F. Jaiser, D. Spoltore, O. Zeika, Z. Ma, D. Neher, K. Vandewal, and K. Leoa, "Boron dipyrromethene (BODIPY) with meso-perfluorinated alkyl substituents as near infrared donors in organic solar cells," *J. Mater. Chem. A* **6**, 18583–18591 (2018).
- ³⁴G. Kumar, R. S. Pillai, N.-u H. Khan, and S. Neogi, "Structural engineering in pre-functionalized, imine-based covalent organic framework via anchoring active Ru(II)-complex for visible-light triggered and aerobic cross-coupling of α -amino esters with indoles," *Appl. Catal., B* **292**, 120149 (2021).
- ³⁵H. G. Cha and K. S. Choi, "Combined biomass valorization and hydrogen production in a photoelectrochemical cell," *Nat. Chem.* **7**(4), 328–333 (2015).
- ³⁶T. P. Yoon, M. A. Ischay, and J. Du, "Visible light photocatalysis as a greener approach to photochemical synthesis," *Nat. Chem.* **2**(7), 527–532 (2010).
- ³⁷T. Nagasaka, H. Sotome, S. Morikawa, L. M. Uriarte, M. Sliwa, T. Kawai, and H. Miyasaka, "Restriction of the conrotatory motion in photo-induced 6π electrocyclic reaction: Formation of the excited state of the closed-ring isomer in the cyclization," *RSC Adv.* **10**(34), 20038–20045 (2020).
- ³⁸D. P. Hari and B. König, "Synthetic applications of eosin Y in photoredox catalysis," *Chem. Commun.* **50**(51), 6688–6699 (2014).
- ³⁹B. Yi, X. Wen, Z. Yi, Y. Xie, Q. Wang, and J.-P. Tan, "Visible-light-enabled regioselective aerobic oxidative C(sp²)-H thiocyanation of aromatic compounds by Eosin-Y photocatalyst," *Tetrahedron Lett.* **61**(50), 152628 (2020).
- ⁴⁰H. Ni, Y. Li, X. Shi, Y. Pang, C. Jin, and F. Zhao, "Eosin Y as a direct hydrogen-atom transfer photocatalyst for the C3-H acylation of quinoxalin-2 (1H)-ones," *Tetrahedron Lett.* **68**, 152915 (2021).
- ⁴¹N. A. Romero and D. A. Nicewicz, "Organic photoredox catalysis," *Chem. Rev.* **116**(17), 10075–10166 (2016).
- ⁴²Y. Li, X. Li, H. Zhang, and Q. Xiang, "Porous graphitic carbon nitride for solar photocatalytic applications," *Nanoscale Horiz.* **5**(5), 765–786 (2020).
- ⁴³K. J. Mintz, M. Bartoli, M. Rovere, Y. Zhou, S. D. Hettiarachchi, S. Paudyal, J. Chen, J. B. Domena, P. Y. Liyanage, R. Sampson, D. Khadka, R. R. Pandey, S. Huang, C. C. Chusuei, A. Tagliaferro, and R. M. Leblanc, "A deep investigation into the structure of carbon dots," *Carbon* **173**, 433–447 (2021).
- ⁴⁴R. Paul, C. Sarkar, M. Jain, S. Xu, K. Borah, D. Q. Dao, C.-W. Pao, S. Bhattacharya, and J. Mondal, "Ferrocene-derived Fe-metalated porous organic polymer for the core planarity-triggered detoxification of chemical warfare agents," *Chem. Commun.* **58**(56), 7789–7792 (2022).
- ⁴⁵R. Malik and V. K. Tomer, "State-of-the-art review of morphological advancements in graphitic carbon nitride (g-CN) for sustainable hydrogen production," *Renewable Sustainable Energy Rev.* **135**, 110235 (2021).
- ⁴⁶A. Pal, M. P. Sk, and A. Chattopadhyay, "Recent advances in crystalline carbon dots for superior application potential," *Mater. Adv.* **1**(4), 525–553 (2020).
- ⁴⁷C. Hu, M. Li, J. Qiu, and Y.-P. Sun, "Design and fabrication of carbon dots for energy conversion and storage," *Chem. Soc. Rev.* **48**(8), 2315–2337 (2019).
- ⁴⁸J. Kosco, S. Gonzalez-Carrero, C. T. Howells, T. Fei, Y. Dong, R. Sougrat, G. T. Harrison, Y. Firdaus, R. Sheelamanthula, B. Purushothaman, F. Moruzzi, W. Xu, L. Zhao, A. Basu, S. D. Wolf, T. D. Anthopoulos, J. R. Durrant, and I. McCulloch, "Generation of long-lived charges in organic semiconductor heterojunction nanoparticles for efficient photocatalytic hydrogen evolution," *Nat. Energy* **7**, 340–351 (2022).
- ⁴⁹L. Ai, R. Shi, J. Yang, K. Zhang, T. Zhang, and S. Lu, "Efficient combination of g-C₃N₄ and CDs for enhanced photocatalytic performance: A review of synthesis, strategies, and applications," *Small* **17**(48), 2007523 (2021).
- ⁵⁰M. L. Liu, B. B. Chen, C. M. Li, and C. Z. Huang, "Carbon dots: Synthesis, formation mechanism, fluorescence origin and sensing applications," *Green Chem.* **21**(3), 449–471 (2019).
- ⁵¹G. Ge, L. Li, D. Wang, M. Chen, Z. Zeng, W. Xiong, X. Wu, and C. Guo, "Carbon dots: Synthesis, properties and biomedical applications," *J. Mater. Chem. B* **9**, 6553 (2021).
- ⁵²N. Tian, Y. Zhang, X. Li, K. Xiao, X. Du, F. Dong, G. I. N. Waterhouse, T. Zhang, and H. Huang, "Precursor-reforming protocol to 3D mesoporous g-C₃N₄ established by ultrathin self-doped nanosheets for superior hydrogen evolution," *Nano Energy* **38**, 72–81 (2017).
- ⁵³Z. Chen, K. O. Kirlikovali, K. B. Idrees, M. C. Wasson, and O. K. Farha, "Porous materials for hydrogen storage," *Chem* **8**(3), 693–716 (2022).
- ⁵⁴L. Jiang, X. Yuan, Y. Pan, J. Liang, G. Zeng, Z. Wu, and H. Wang, "Doping of graphitic carbon nitride for photocatalysis: A review," *Appl. Catal., B* **217**, 388–406 (2017).
- ⁵⁵H. Yu, R. Shi, Y. Zhao, G. I. N. Waterhouse, L.-Z. Wu, C.-H. Tung, and T. Zhang, "Smart utilization of carbon dots in semiconductor photocatalysis," *Adv. Mater.* **28**(43), 9454–9477 (2016).
- ⁵⁶P. B. Pati, G. Damas, L. Tian, D. L. A. Fernandes, L. Zhang, I. B. Pehlivan, T. Edvinsson, C. M. Araujo, and H. Tian, "An experimental and theoretical study of an efficient polymer nano-photocatalyst for hydrogen evolution," *Energy Environ. Sci.* **10**, 1372–1376 (2017).
- ⁵⁷Z. Zhang, J. Jia, Y. Zhi, S. Ma, and X. Liu, "Porous organic polymers for light-driven organic transformations," *Chem. Soc. Rev.* **51**(7), 2444–2490 (2022).
- ⁵⁸C. Sarkar, S. C. Shit, N. Das, and J. Mondal, "Presenting porous-organic-polymers as next-generation invigorating materials for nanoreactors," *Chem. Commun.* **57**(69), 8550–8567 (2021).
- ⁵⁹X. Li, X. Ma, F. Zhang, X. Dong, and X. Lang, "Selective photocatalytic formation of sulfoxides by aerobic oxidation of sulfides over conjugated microporous polymers with thiazolo [5,4-d]thiazole linkage," *Appl. Catal., B* **298**, 120514 (2021).
- ⁶⁰Y.-Z. Cheng, X. Ding, and B.-H. Han, "Porous organic polymers for photocatalytic carbon dioxide reduction," *Chemphotochem* **5**(5), 406–417 (2021).
- ⁶¹Z. J. Wang, K. Garth, S. Ghasimi, K. Landfester, and K. A. I. Zhang, "Conjugated microporous poly(benzochalcogenadiazole)s for photocatalytic oxidative coupling of amines under visible light," *ChemSuschem* **8**(20), 3459–3464 (2015).
- ⁶²V. R. Battula, H. Singh, S. Kumar, I. Bala, S. K. Pal, and K. Kailasam, "Natural sunlight driven oxidative homocoupling of amines by a truxene-based conjugated microporous polymer," *ACS Catal.* **8**(8), 6751–6759 (2018).
- ⁶³R. Wang, C. Zhou, X. Huang, J.-Y. Wu, and X. Zhang, "Phenylphenothiazine-based porous organic polymers as visible-light heterogeneous photocatalysts for switchable bromoalkylation and cyclopropanation of unactivated terminal alkenes," *ACS Sustainable Chem. Eng.* **10**(14), 4650–4659 (2022).
- ⁶⁴F. Yang, C.-C. Li, C.-C. Xu, J.-L. Kan, B. Tian, H.-Y. Qu, Y. Guo, Y. Geng, and Y.-B. Dong, "A covalent organic framework as a photocatalyst for window ledge cross-dehydrogenative coupling reactions," *Chem. Commun.* **58**(10), 1530–1533 (2022).
- ⁶⁵F. Unglaube, P. Hünemörder, X. Guo, Z. Chen, D. Wang, and E. Mejía, "Phenazine radical cations as efficient homogeneous and heterogeneous catalysts for the cross-dehydrogenative aza-Henry reaction," *Helv. Chim. Acta* **103**(12), e2000184 (2020).
- ⁶⁶W. Zhang, J. Tang, W. Yu, Q. Huang, Y. Fu, G. Kuang, C. Pan, and G. Yu, "Visible light-driven C-3 functionalization of indoles over conjugated microporous polymers," *ACS Catal.* **8**(9), 8084–8091 (2018).

- ⁶⁷Z. Li, S. Han, C. Li, P. Shao, H. Xia, H. Li, X. Chen, X. Feng, and X. Liu, "Screening metal-free photocatalysts from isomorphous covalent organic frameworks for the C-3 functionalization of indoles," *J. Mater. Chem. A* **8**(17), 8706–8715 (2020).
- ⁶⁸W. Zhang, H. Zuo, Z. Cheng, Y. Shi, Z. Guo, N. Meng, A. Thomas, and Y. Liao, "Macroscale conjugated microporous polymers: Controlling versatile functionalities over several dimensions," *Adv. Mater.* **34**(18), 2104952 (2022).
- ⁶⁹J.-S. M. Lee and A. I. Cooper, "Advances in conjugated microporous polymers," *Chem. Rev.* **120**(4), 2171–2214 (2020).
- ⁷⁰Y. Xu, S. Jin, H. Xu, A. Nagai, and D. Jiang, "Conjugated microporous polymers: Design, synthesis and application," *Chem. Soc. Rev.* **42**(20), 8012–8031 (2013).
- ⁷¹S. Luo, Z. Zeng, H. Wang, W. Xiong, B. Song, C. Zhou, A. Duan, X. Tan, Q. He, G. Zeng, Z. Liu, and R. Xiao, "Recent progress in conjugated microporous polymers for clean energy: Synthesis, modification, computer simulations, and applications," *Prog. Polym. Sci.* **115**, 101374 (2021).
- ⁷²G. E. M. Schukraft, R. T. Woodward, S. Kumar, M. Sachs, S. Eslava, and C. Petit, "Hypercrosslinked polymers as a photocatalytic platform for visible-light-driven CO₂ photoreduction using H₂O," *Chemsuschem* **14**(7), 1720–1727 (2021).
- ⁷³J. Huang and S. R. Turner, "Hypercrosslinked polymers: A review," *Polym. Rev.* **58**(1), 1–41 (2018).
- ⁷⁴S. J. Choi, E. H. Choi, C. Song, Y.-J. Ko, S. M. Lee, H. J. Kim, H.-Y. Jang, and S. U. Son, "Hyper-cross-linked polymer on the hollow conjugated microporous polymer platform: A heterogeneous catalytic system for poly(caprolactone) synthesis," *ACS Macro Lett.* **8**(6), 687–693 (2019).
- ⁷⁵L. Tan and B. Tan, "Hypercrosslinked porous polymer materials: Design, synthesis, and applications," *Chem. Soc. Rev.* **46**(11), 3322–3356 (2017).
- ⁷⁶F. Marken, M. Carta, and N. B. McKeown, "Polymers of intrinsic microporosity in the design of electrochemical multicomponent and multiphase interfaces," *Anal. Chem.* **93**(3), 1213–1220 (2021).
- ⁷⁷P. M. Budd, B. S. Ghanem, S. Makhseed, N. B. McKeown, K. J. Msayib, and C. E. Tattershall, "Polymers of intrinsic microporosity (PIMs): Robust, solution-processable, organic nanoporous materials," *Chem. Commun.* **2004**, 230–231.
- ⁷⁸Y. Wang, B. S. Ghanem, Z. Ali, K. Hazazi, Y. Han, and I. Pinnau, "Recent progress on polymers of intrinsic microporosity and thermally modified analogue materials for membrane-based fluid separations," *Small Struct.* **2**(9), 2100049 (2021).
- ⁷⁹Y. Yuan, Y. Yang, and G. Zhu, "Multifunctional porous aromatic frameworks: State of the art and opportunities," *Energymchem* **2**(5), 100037 (2020).
- ⁸⁰Y. Tian and G. Zhu, "Porous aromatic frameworks (PAFs)," *Chem. Rev.* **120**(16), 8934–8986 (2020).
- ⁸¹E. Rangel-Rangel, E. Verde-Sesto, A. M. Rasero-Almansa, M. Iglesias, and F. Sánchez, "Porous aromatic frameworks (PAFs) as efficient supports for N-heterocyclic carbene catalysts," *Catal. Sci. Technol.* **6**(15), 6037–6045 (2016).
- ⁸²L.-M. Tao, F. Niu, D. Zhang, T.-M. Wang, and Q.-H. Wang, "Amorphous covalent triazine frameworks for high performance room temperature ammonia gas sensing," *New J. Chem.* **38**(7), 2774–2777 (2014).
- ⁸³K. Geng, T. He, R. Liu, S. Dalapati, K. T. Tan, Z. Li, S. Tao, Y. Gong, Q. Jiang, and D. Jiang, "Covalent organic frameworks: Design, synthesis, and functions," *Chem. Rev.* **120**(16), 8814–8933 (2020).
- ⁸⁴W. Zhang, L. Chen, S. Dai, C. Zhao, C. Ma, L. Wei, M. Zhu, S. Y. Chong, H. Yang, L. Liu, Y. Bai, M. Yu, Y. Xu, X.-W. Zhu, Q. Zhu, S. An, R. S. Sprick, M. A. Little, X. Wu, S. Jiang, Y. Wu, Y.-B. Zhang, H. Tian, W.-H. Zhu, and A. I. Cooper, "Reconstructed covalent organic frameworks," *Nature* **604**(7904), 72–79 (2022).
- ⁸⁵R. K. Sharma, P. Yadav, M. Yadav, R. Gupta, P. Rana, A. Srivastava, R. Zboril, R. S. Varma, M. Antonietti, and M. B. Gawande, "Recent development of covalent organic frameworks (COFs): Synthesis and catalytic (organic-electro-photo) applications," *Mater. Horiz.* **7**(2), 411–454 (2020).
- ⁸⁶C. S. Diercks and O. M. Yaghi, "The atom, the molecule, and the covalent organic framework," *Science* **355**(6328), eaal1585 (2017).
- ⁸⁷C. Wang, Z. Zhang, Y. Zhu, C. Yang, J. Wu, and W. Hu, "2D covalent organic frameworks: From synthetic strategies to advanced optical-electrical-magnetic functionalities," *Adv. Mater.* **34**(17), 2102290 (2022).
- ⁸⁸M. Liu, L. Guo, S. Jin, and B. Tan, "Covalent triazine frameworks: Synthesis and applications," *J. Mater. Chem. A* **7**(10), 5153–5172 (2019).
- ⁸⁹Z. Qian, Z. J. Wang, and K. A. I. Zhang, "Covalent triazine frameworks as emerging heterogeneous photocatalysts," *Chem. Mater.* **33**(6), 1909–1926 (2021).
- ⁹⁰X. Hu, Z. Zhan, J. Zhang, I. Hussain, and B. Tan, "Immobilized covalent triazine frameworks films as effective photocatalysts for hydrogen evolution reaction," *Nat. Commun.* **12**(1), 6596 (2021).
- ⁹¹R. Luo, W. Xu, M. Chen, X. Liu, Y. Fang, and H. Ji, "Covalent triazine frameworks obtained from nitrile monomers for sustainable CO₂ catalysis," *Chemsuschem* **13**(24), 6509–6522 (2020).
- ⁹²J. L. Segura, S. Royuela, and M. Mar Ramos, "Post-synthetic modification of covalent organic frameworks," *Chem. Soc. Rev.* **48**(14), 3903–3945 (2019).
- ⁹³T. Ratvijitvech, R. Dawson, A. Laybourn, Y. Z. Khimyak, D. J. Adams, and A. I. Cooper, "Post-synthetic modification of conjugated microporous polymers," *Polymers* **55**(1), 321–325 (2014).
- ⁹⁴H. Ding, A. Mal, and C. Wang, "Tailored covalent organic frameworks by post-synthetic modification," *Mater. Chem. Front.* **4**(1), 113–127 (2020).
- ⁹⁵Z. J. Wang, S. Ghasimi, K. Landfester, and K. A. I. Zhang, "Highly porous conjugated polymers for selective oxidation of organic sulfides under visible light," *Chem. Commun.* **50**(60), 8177–8180 (2014).
- ⁹⁶H.-K. Liu, Y.-F. Lei, P.-J. Tian, H. Wang, X. Zhao, Z.-T. Li, and D.-W. Zhang, "Fe(bpy)₃2+-based porous organic polymers with boosted photocatalytic activity for recyclable organic transformations," *J. Mater. Chem. A* **9**(10), 6361–6367 (2021).
- ⁹⁷S. Liu, Z. Liu, Q. Su, and Q. Wu, "Multifunctional covalent organic frameworks for photocatalytic oxidative hydroxylation of arylboronic acids and fluorescence sensing for Cu²⁺," *Microporous Mesoporous Mater.* **333**, 111737 (2022).
- ⁹⁸X. Guo, J. Rabeah, R. Sun, D. Wang, and E. Mejía, "Fluorescent hybrid porous polymers as sustainable heterogeneous photocatalysts for cross-dehydrogenative coupling reactions," *ACS Appl. Mater. Interfaces* **13**(36), 42889–42897 (2021).
- ⁹⁹G. Kumar, S. R. Dash, and S. Neogi, "Dual-catalyst engineered porous organic framework for visible-light triggered, metal-free and aerobic sp³ CH activation in highly synergistic and recyclable fashion," *J. Catal.* **394**, 40–49 (2021).
- ¹⁰⁰Y. Zhi, S. Ma, H. Xia, Y. Zhang, Z. Shi, Y. Mu, and X. Liu, "Construction of donor-acceptor type conjugated microporous polymers: A fascinating strategy for the development of efficient heterogeneous photocatalysts in organic synthesis," *Appl. Catal., B* **244**, 36–44 (2019).
- ¹⁰¹W. Gong, X. Deng, K. Dong, L. Liu, and G. Ning, "A boronil-based conjugated microporous polymer for efficient visible-light-driven heterogeneous photocatalysis," *Polym. Chem.* **12**(21), 3153–3159 (2021).
- ¹⁰²J. Luo, J. Lu, and J. Zhang, "Carbazole-triazine based donor-acceptor porous organic frameworks for efficient visible-light photocatalytic aerobic oxidation reactions," *J. Mater. Chem. A* **6**(31), 15154–15161 (2018).
- ¹⁰³C. Su, R. Tandiana, B. Tian, A. Sengupta, W. Tang, J. Su, and K. P. Loh, "Visible-light photocatalysis of aerobic oxidation reactions using carbazolic conjugated microporous polymers," *ACS Catal.* **6**(6), 3594–3599 (2016).
- ¹⁰⁴W. Huang, B. C. Ma, H. Lu, R. Li, L. Wang, K. Landfester, and K. A. I. Zhang, "Visible-light-promoted selective oxidation of alcohols using a covalent triazine framework," *ACS Catal.* **7**(8), 5438–5442 (2017).
- ¹⁰⁵S. P. Pitre, C. D. McTiernan, H. Ismaili, and J. C. Scaiano, "Mechanistic insights and kinetic analysis for the oxidative hydroxylation of arylboronic acids by visible light photoredox catalysis: A metal-free alternative," *J. Am. Chem. Soc.* **135**(36), 13286–13289 (2013).
- ¹⁰⁶J. Luo, X. Zhang, and J. Zhang, "Carbazolic porous organic framework as an efficient, metal-free visible-light photocatalyst for organic synthesis," *ACS Catal.* **5**(4), 2250–2254 (2015).
- ¹⁰⁷D. Vasudevan and H. Wendt, "Electroreduction of oxygen in aprotic media," *J. Electroanal. Chem.* **392**(1), 69–74 (1995).
- ¹⁰⁸Y. Nailwal, A. D. D. Wananke, M. A. Addicoat, and S. K. Pal, "A dual-function highly crystalline covalent organic framework for HCl sensing and visible-light heterogeneous photocatalysis," *Macromolecules* **54**(13), 6595–6604 (2021).
- ¹⁰⁹Y.-Z. Cheng, W. Ji, X. Wu, X. Ding, X.-F. Liu, and B.-H. Han, "Persistent radical cation sp² carbon-covalent organic framework for photocatalytic oxidative organic transformations," *Appl. Catal., B* **306**, 121110 (2022).

- ¹¹⁰X. Wang, C. Wang, H.-Q. Tan, T.-Y. Qiu, Y.-M. Xing, Q.-K. Shang, Y.-N. Zhao, X.-Y. Zhao, and Y.-G. Li, "Design of porous organic polymer photocatalysts based on heptazine for efficient photocatalytic aerobic oxidation," *Chem. Eng. J.* **431**, 134051 (2022).
- ¹¹¹M. Bhadra, S. Kandambeth, M. K. Sahoo, M. Addicoat, E. Balaraman, and R. Banerjee, "Triazine functionalized porous covalent organic framework for photo-organocatalytic E-Z isomerization of olefins," *J. Am. Chem. Soc.* **141**(15), 6152–6156 (2019).
- ¹¹²Z. J. Wang, S. Ghasimi, K. Landfester, and K. A. I. Zhang, "A conjugated porous poly-benzobisthiadiazole network for a visible light-driven photoredox reaction," *J. Mater. Chem. A* **2**(44), 18720–18724 (2014).
- ¹¹³W. Huang, Z. J. Wang, B. C. Ma, S. Ghasimi, D. Gehrig, F. Laquai, K. Landfester, and K. A. I. Zhang, "Hollow nanoporous covalent triazine frameworks via acid vapor-assisted solid phase synthesis for enhanced visible light photoactivity," *J. Mater. Chem. A* **4**(20), 7555–7559 (2016).
- ¹¹⁴M. Kropp and G. B. Schuster, "Photoreduction of substituted arenes with borates and borohydride: An electron transfer mechanism," *Tetrahedron Lett.* **28**(44), 5295–5298 (1987).
- ¹¹⁵J. Liebig, "About some nitrogen compounds," *Ann. Pharm.* **10**(10), 1–47 (1834).
- ¹¹⁶E. C. Franklin, "The ammonio carbonic acids," *J. Am. Chem. Soc.* **44**(3), 486–509 (1922).
- ¹¹⁷X. Wang, K. Maeda, A. Thomas, K. Takanabe, G. Xin, J. M. Carlsson, K. Domen, and M. Antonietti, "A metal-free polymeric photocatalyst for hydrogen production from water under visible light," *Nat. Mater.* **8**(1), 76–80 (2009).
- ¹¹⁸Y. Wang, X. Wang, and M. Antonietti, "Polymeric graphitic carbon nitride as a heterogeneous organocatalyst: From photochemistry to multipurpose catalysis to sustainable chemistry," *Angew. Chem. Int. Ed.* **51**(1), 68–89 (2012).
- ¹¹⁹A. Thomas, A. Fischer, F. Goettmann, M. Antonietti, J.-O. Müller, R. Schlögl, and J. M. Carlsson, "Graphitic carbon nitride materials: Variation of structure and morphology and their use as metal-free catalysts," *J. Mater. Chem.* **18**(41), 4893–4908 (2008).
- ¹²⁰W. Wu, J. Zhang, W. Fan, Z. Li, L. Wang, X. Li, Y. Wang, R. Wang, J. Zheng, M. Wu, and H. Zeng, "Remediating defects in carbon nitride to improve both photo-oxidation and H₂ generation efficiencies," *ACS Catal.* **6**(5), 3365–3371 (2016).
- ¹²¹Y. Cui, G. Zhang, Z. Lin, and X. Wang, "Condensed and low-defected graphitic carbon nitride with enhanced photocatalytic hydrogen evolution under visible light irradiation," *Appl. Catal., B* **181**, 413–419 (2016).
- ¹²²W.-J. Ong, L.-L. Tan, Y. H. Ng, S.-T. Yong, and S.-P. Chai, "Graphitic carbon nitride (g-C₃N₄)-based photocatalysts for artificial photosynthesis and environmental remediation: Are we a step closer to achieving sustainability?," *Chem. Rev.* **116**(12), 7159–7329 (2016).
- ¹²³A. Mishra, A. Mehta, S. Basu, N. P. Shetti, K. R. Reddy, and T. M. Aminabhavi, "Graphitic carbon nitride (g-C₃N₄)-based metal-free photocatalysts for water splitting: A review," *Carbon* **149**, 693–721 (2019).
- ¹²⁴X. Chen, R. Shi, Q. Chen, Z. Zhang, W. Jiang, Y. Zhu, and T. Zhang, "Three-dimensional porous g-C₃N₄ for highly efficient photocatalytic overall water splitting," *Nano Energy* **59**, 644–650 (2019).
- ¹²⁵W. Che, W. Cheng, T. Yao, F. Tang, W. Liu, H. Su, Y. Huang, Q. Liu, J. Liu, F. Hu, Z. Pan, Z. Sun, and S. Wei, "Fast photoelectron transfer in (Cring)-C₃N₄ plane heterostructural nanosheets for overall water splitting," *J. Am. Chem. Soc.* **139**(8), 3021–3026 (2017).
- ¹²⁶X. Liu, R. Ma, L. Zhuang, B. Hu, J. Chen, X. Liu, and X. Wang, "Recent developments of doped g-C₃N₄ photocatalysts for the degradation of organic pollutants," *Crit. Rev. Environ. Sci. Technol.* **51**(8), 751–790 (2021).
- ¹²⁷X. Yang, Y. Ye, J. Sun, Z. Li, J. Ping, and X. Sun, "Recent advances in g-C₃N₄-based photocatalysts for pollutant degradation and bacterial disinfection: Design strategies, mechanisms, and applications," *Small* **18**(9), 2105089 (2022).
- ¹²⁸K. Wang, Q. Li, B. S. Liu, B. Cheng, W. K. Ho, and J. G. Yu, "Sulfur-doped g-C₃N₄ with enhanced photocatalytic CO₂-reduction performance," *Appl. Catal., B* **176**, 44–52 (2015).
- ¹²⁹J. W. Fu, B. C. Zhu, C. J. Jiang, B. Cheng, W. You, and J. G. Yu, "Hierarchical porous O-doped g-C₃N₄ with enhanced photocatalytic CO₂ reduction activity," *Small* **13**(15), 1603938 (2017).
- ¹³⁰X. F. Chen, J. S. Zhang, X. Z. Fu, M. Antonietti, and X. C. Wang, "Fe-g-C₃N₄-catalyzed oxidation of benzene to phenol using hydrogen peroxide and visible light," *J. Am. Chem. Soc.* **131**(33), 11658 (2009).
- ¹³¹G. Marci, E. I. García-López, F. R. Pomilla, L. Palmisano, A. Zaffora, M. Santamaria, I. Krivtsov, M. Ilkaeva, Z. Barbieriková, and V. Brezová, "Photoelectrochemical and EPR features of polymeric C₃N₄ and O-modified C₃N₄ employed for selective photocatalytic oxidation of alcohols to aldehydes," *Catal. Today* **328**(15), 21–28 (2019).
- ¹³²M. Bellardita, E. I. García-López, G. Marci, I. Krivtsov, J. R. García, and L. Palmisano, "Selective photocatalytic oxidation of aromatic alcohols in water by using P-doped g-C₃N₄," *Appl. Catal., B* **220**, 222–233 (2018).
- ¹³³F. Su, S. C. Mathew, G. Lipner, X. Fu, M. Antonietti, S. Blechert, and X. Wang, "mpg-C(3)N(4)-Catalyzed selective oxidation of alcohols using O(2) and visible light," *J. Am. Chem. Soc.* **132**(46), 16299–16301 (2010).
- ¹³⁴C. Xiao, L. Zhang, H. Hao, and W. Wang, "High selective oxidation of benzyl alcohol to benzaldehyde and benzoic acid with surface oxygen vacancies on W₁₈O₄₉/holey ultrathin g-C₃N₄ nanosheets," *ACS Sustainable Chem. Eng.* **7**(7), 7268–7276 (2019).
- ¹³⁵S. Juntapirom, S. Anuchai, O. Thongsook, S. Pornsuwan, P. Meepowpan, P. Thavornutikarn, S. Phanichphant, D. Tantraviwat, and B. Inceesungvorn, "Photocatalytic activity enhancement of g-C₃N₄/BiOBr in selective transformation of primary amines to imines and its reaction mechanism," *Chem. Eng. J.* **394**, 124934 (2020).
- ¹³⁶Y. Y. Chai, L. Zhang, Q. Q. Liu, F. L. Yang, and W. L. Dai, "Insights into the relationship of the heterojunction structure and excellent activity: Photo-oxidative coupling of benzylamine on CeO₂-rod/g-C₃N₄ hybrid under mild reaction conditions," *ACS Sustainable Chem. Eng.* **6**(8), 10526–10535 (2018).
- ¹³⁷S. Samanta, S. Khilari, D. Pradhan, and R. Srivastava, "An efficient, visible light driven, selective oxidation of aromatic alcohols and amines with O₂ using BiVO₄/g-C₃N₄ nanocomposite: A systematic and comprehensive study toward the development of a photocatalytic process," *ACS Sustainable Chem. Eng.* **5**(3), 2562–2577 (2017).
- ¹³⁸Q. Qi, Y. Li, H. Liu, B. Li, H. Wang, Y. Lu, W. Gao, Y. Tian, B. Guo, X. Jia, and J. Chen, "Alkali metal modified carbon nitride enhance photocatalytic performance for highly selective oxidation of benzyl C(sp³)-H bonds," *Appl. Catal., B* **319**, 121864 (2022).
- ¹³⁹S. Das, K. Murugesan, G. J. Villegas Rodríguez, J. Kaur, J. P. Barham, A. Savateev, M. Antonietti, and B. König, "Photocatalytic (Het)arylation of C(sp³)-H bonds with carbon nitride," *ACS Catal.* **11**(3), 1593–1603 (2021).
- ¹⁴⁰X.-H. Li, M. Baar, S. Blechert, and M. Antonietti, "Facilitating room-temperature Suzuki coupling reaction with light: Mott-Schottky photocatalyst for C-C-coupling," *Sci. Rep.* **3**(1), 1743 (2013).
- ¹⁴¹C. Han, R. Qi, R. Sun, K. Fan, B. Johannessen, D.-C. Qi, S. Cao, and J. Xu, "Enhanced support effects in single-atom copper-incorporated carbon nitride for photocatalytic Suzuki cross-coupling reactions," *Appl. Catal., B* **320**, 121954 (2023).
- ¹⁴²X. T. Tian and X. B. Yin, "Carbon dots, unconventional preparation strategies, and applications beyond photoluminescence," *Small* **15**(48), 1901803 (2019).
- ¹⁴³L. Guo, J. Ge, W. Liu, G. Niu, Q. Jia, H. Wang, and P. Wang, "Tunable multi-color carbon dots prepared from well-defined polythiophene derivatives and their emission mechanism," *Nanoscale* **8**(2), 729–734 (2016).
- ¹⁴⁴X. Wang, L. Cao, S. T. Yang, F. Lu, M. J. Mezziani, L. Tian, K. W. Sun, M. A. Bloodgood, and Y. P. Sun, "Bandgap-like strong fluorescence in functionalized carbon nanoparticles," *Angew. Chem. Int. Ed.* **49**(31), 5310–5314 (2010).
- ¹⁴⁵S. Zarezaadeh, A. Habibi-Yangjeh, and M. Mousavi, "Fabrication of novel ZnO/BiOBr/C-dots nanocomposites with considerable photocatalytic performances in removal of organic pollutants under visible light," *Adv. Powder Technol.* **30**(6), 1197–1209 (2019).
- ¹⁴⁶Y. Li, X. Feng, Z. Lu, H. Yin, F. Liu, and Q. Xiang, "Enhanced photocatalytic H₂-production activity of C-dots modified g-C₃N₄/TiO₂ nanosheets composites," *J. Colloid Interface Sci.* **513**, 866–876 (2018).
- ¹⁴⁷H. Ming, Z. Ma, Y. Liu, K. M. Pan, H. Yu, F. Wang, and Z. H. Kang, "Large scale electrochemical synthesis of high quality carbon nanodots and their photocatalytic property," *Dalton Trans.* **41**(31), 9526–9531 (2012).
- ¹⁴⁸D. Xu, Q. Lin, and H. T. Chang, "Recent advances and sensing applications of carbon dots," *Small Methods* **4**(4), 1900387 (2020).

- ¹⁴⁹A. D. Zhao, Z. W. Chen, C. Q. Zhao, N. Gao, J. S. Ren, and X. G. Qu, "Recent advances in bioapplications of C-dots," *Carbon* **85**, 309–327 (2015).
- ¹⁵⁰L. Shen, M. Chen, L. Hu, X. Chen, and J. Wang, "Growth and stabilization of silver nanoparticles on carbon dots and sensing application," *Langmuir* **29**(52), 16135–16140 (2013).
- ¹⁵¹C. Ding, A. Zhu, and Y. Tian, "Functional surface engineering of C-dots for fluorescent biosensing and *in vivo* bioimaging," *Acc. Chem. Res.* **47**(1), 20–30 (2014).
- ¹⁵²C. K. Jiang, H. Wu, X. J. Song, X. J. Ma, J. H. Wang, and M. Q. Tan, "Presence of photoluminescent carbon dots in Nescafe[®] original instant coffee: Applications to bioimaging," *Talanta* **127**, 68–74 (2014).
- ¹⁵³Y. Q. Zhang and R. Wang, "Synthesis of silica@C-dots/phosphotungstates core-shell microsphere for effective oxidative-adsorptive desulfurization of dibenzothiophene with less oxidant," *Appl. Catal., B* **234**, 247–259 (2018).
- ¹⁵⁴P. Fan, X. J. Zhang, H. H. Deng, and X. H. Guan, "Enhanced reduction of p-nitrophenol by zerovalent iron modified with carbon quantum dots," *Appl. Catal., B* **285**, 119829 (2021).
- ¹⁵⁵J. H. Park, F. Raza, S.-J. Jeon, D. Yim, H.-I. Kim, T. W. Kang, and J.-H. Kim, "Oxygen-mediated formation of MoS_x-doped hollow carbon dots for visible light-driven photocatalysis," *J. Mater. Chem. A* **4**(38), 14796–14803 (2016).
- ¹⁵⁶D. Sarma, B. Majumdar, and T. K. Sarma, "Visible-light induced enhancement in the multi-catalytic activity of sulfated carbon dots for aerobic carbon-carbon bond formation," *Green Chem.* **21**(24), 6717–6726 (2019).
- ¹⁵⁷Z. X. Liu, B. B. Chen, M. L. Liu, H. Y. Zou, and C. Z. Huang, "Cu (I)-doped carbon quantum dots with zigzag edge structures for highly efficient catalysis of azide-alkyne cycloadditions," *Green Chem.* **19**(6), 1494–1498 (2017).
- ¹⁵⁸H. Li, R. Liu, S. Lian, Y. Liu, H. Huang, and Z. Kang, "Near-infrared light controlled photocatalytic activity of carbon quantum dots for highly selective oxidation reaction," *Nanoscale* **5**(8), 3289–3297 (2013).
- ¹⁵⁹Y.-Y. Chai, D.-P. Qu, D.-K. Ma, W. Chen, and S. Huang, "Carbon quantum dots/Zn²⁺ ions doped-CdS nanowires with enhanced photocatalytic activity for reduction of 4-nitroaniline to p-phenylenediamine," *Appl. Surf. Sci.* **450**, 1–8 (2018).
- ¹⁶⁰M. Liu, R. Wang, B. Liu, F. Guo, and L. Tian, "Carbon quantum dots@ Pd-SnS₂ nanocomposite: The role of CQDs@Pd nanoclusters in enhancing photocatalytic reduction of aromatic nitro compounds," *J. Colloid Interface Sci.* **555**, 423–430 (2019).
- ¹⁶¹T. Sun and Z. Xie, "Conjugated polymers and polymer dots for cell imaging," in *Fluorescent Materials for Cell Imaging*, edited by F.-G. Wu (Springer Singapore, Singapore, 2020), pp. 155–180.
- ¹⁶²L. Wang, R. Fernández-Terán, L. Zhang, D. L. A. Fernandes, L. Tian, H. Chen, and H. Tian, "Organic polymer dots as photocatalysts for visible light-driven hydrogen generation," *Angew. Chem. Int. Ed.* **55**(40), 12306–12310 (2016).
- ¹⁶³A. Liu, L. Gedda, M. Axelsson, M. Pavliuk, K. Edwards, L. Hammarstrom, and H. Tian, "Panchromatic ternary polymer dots involving sub-picosecond energy and charge transfer for efficient and stable photocatalytic hydrogen evolution," *J. Am. Chem. Soc.* **143**(7), 2875–2885 (2021).
- ¹⁶⁴J. Kosco, M. Bidwell, H. Cha, T. Martin, C. T. Howells, M. Sachs, D. H. Anjum, S. Gonzalez Lopez, L. Zou, A. Wadsworth, W. Zhang, L. Zhang, J. Tellam, R. Sougrat, F. Laquai, D. M. DeLongchamp, J. R. Durrant, and I. McCulloch, "Enhanced photocatalytic hydrogen evolution from organic semiconductor heterojunction nanoparticles," *Nat. Mater.* **19**(5), 559–565 (2020).
- ¹⁶⁵H. Yang, X. Li, R. S. Sprick, and A. I. Cooper, "Conjugated polymer donor-molecular acceptor nanohybrids for photocatalytic hydrogen evolution," *Chem. Commun.* **56**(50), 6790–6793 (2020).
- ¹⁶⁶S. Wang, B. Cai, and H. Tian, "Efficient generation of hydrogen peroxide and formate by an organic polymer dots photocatalyst in alkaline conditions," *Angew. Chem. Int. Ed.* **61**(23), e202202733 (2022).